Higgs Boson Fiducial Cross Section Measurements in the Four-lepton Final State

Qianying GUO

(Beihang University and Institute of High Energy Physics, Beijing)

On behalf of CMS HZZ4l team

Moriond EW2023, 18-25 Mar 2023, La Thuile (Italy)

Overview

- **Fiducial cross section measurement** [CMS PAS-HIG-21-009] in $H \to ZZ^* \to 4l$ channel with 138fb^{-1} of Run II samples with latest objects calibration
- Extend the measurement with respect to the previous Run II analysis [EPJC81(2021)488]
- **Inclusive fiducial** cross section measurement
- **Differential fiducial** cross section measurements
  - Revised binning and extended set of variables (4 $\Rrightarrow$ **31**)
  - Compared with POWHEG, **MADGRAPH5**, and NNLOPS predictions
  - **1D measurements**
    - Production observables
    - Decay observables
      - Matrix-Element discriminants
  - **2D measurements**
    - Enhance sensitivity to specific phase space regions
- **Interpretations**
  - Higgs boson trilinear self-coupling κ_λ
  - Higgs boson couplings modifier κ_b, κ_c

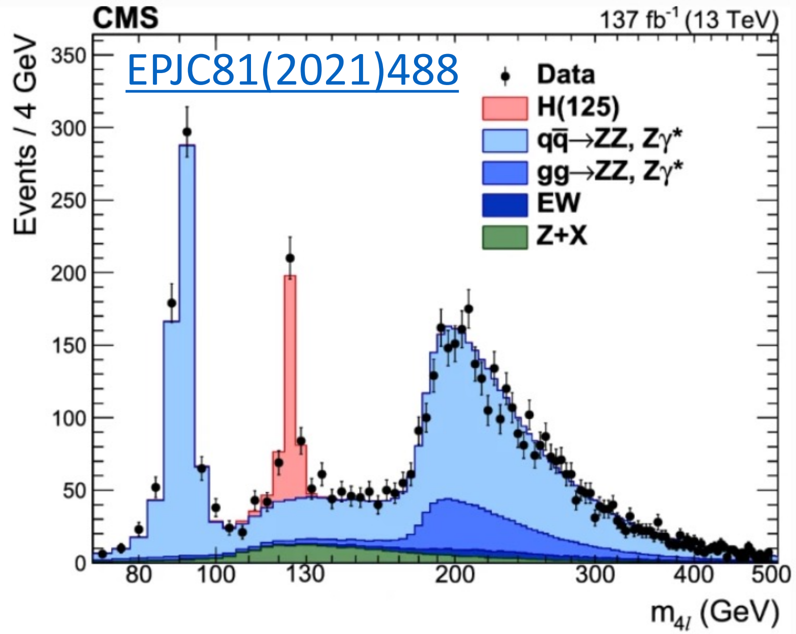

Overview

- **Fiducial cross section measurement** [CMS PAS-HIG-21-009] in $H \rightarrow ZZ^* \rightarrow 4l$ channel with 138fb^{-1} of Run II samples with latest objects calibration
- Extend the measurement with respect to the previous Run II analysis [EPJC81(2021)488]
- **Inclusive fiducial** cross section measurement
- **Differential fiducial** cross section measurements

Requirements for the $H \rightarrow ZZ \rightarrow 4\ell$ fiducial phase space	
Lepton kinematics and isolation	
Leading lepton p_T	$p_T > 20\,\mathrm{GeV}$
Sub-leading lepton p_T	$p_T > 10\,\mathrm{GeV}$
Additional electrons (muons) p_T	$p_T > 7(5)\,\mathrm{GeV}$
Pseudorapidity of electrons (muons)	$\lvert\eta\rvert < 2.5\ (2.4)$
Sum of scalar p_T of all stable particles within $\Delta R < 0.3$ from lepton	$< 0.35 p_T$
Event topology	
Existence of at least two same-flavor OS lepton pairs, where leptons satisfy criteria above	
Inv. mass of the Z_1 candidate	$40 < m_{Z_1} < 120\,\mathrm{GeV}$
Inv. mass of the Z_2 candidate	$12 < m_{Z_2} < 120\,\mathrm{GeV}$
Distance between selected four leptons	$\Delta R(\ell_i, \ell_j) > 0.02$ for any $i \neq j$
Inv. mass of any opposite sign lepton pair	$m_{\ell^+\ell'^-} > 4\,\mathrm{GeV}$
Inv. mass of the selected four leptons	$105 < m_{4\ell} < 160\,\mathrm{GeV}$

Its definition matches closely the experimental acceptance after the reconstruction-level selection.

Results of Inclusive Fiducial Cross Section

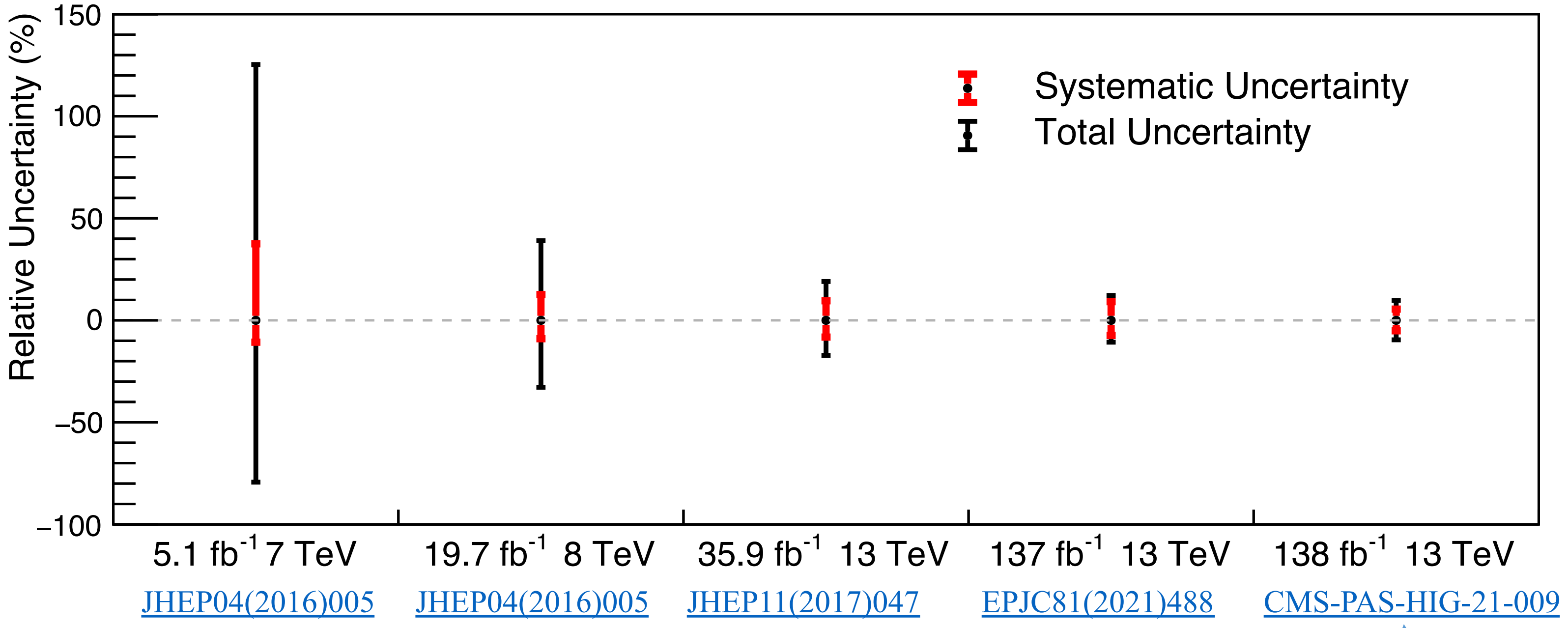

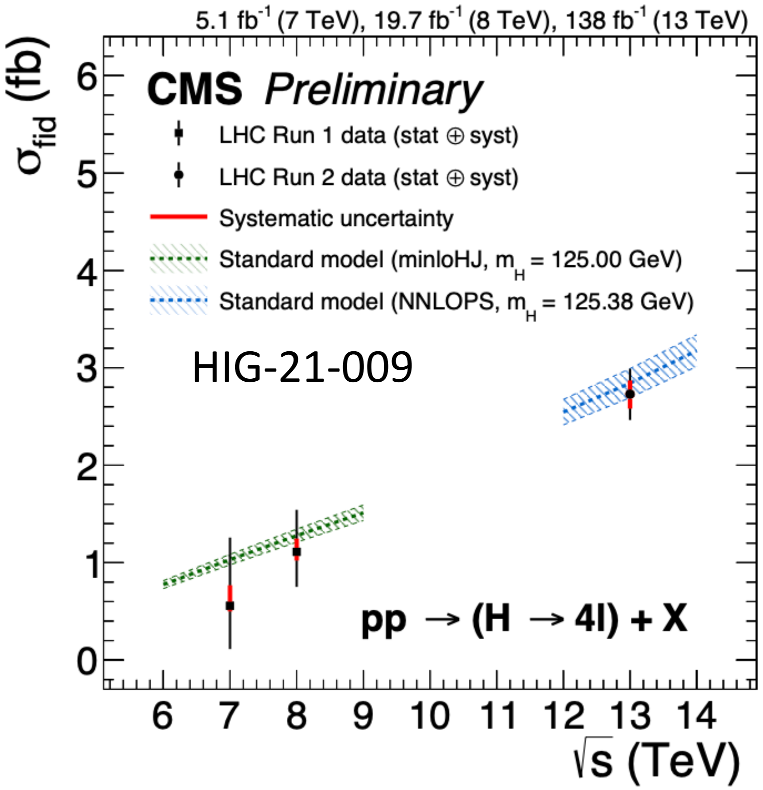

$$\sigma^{\text{fid}} = 2.73^{+0.22}_{-0.22}\,(\text{stat})^{+0.15}_{-0.14}\,(\text{syst})\,\text{fb}$$
$$= 2.73^{+0.22}_{-0.22}\,(\text{stat})^{+0.12}_{-0.12}(\text{electrons})^{+0.06}_{-0.05}(\text{lumi})^{+0.04}_{-0.04}(\text{bkg})^{+0.03}_{-0.02}(\text{muons})\,\text{fb}$$

Fiducial cross section as a function of center of mass

- Systematic uncertainty dominated by
  - Electrons-related nuisances,
  - Especially electron reconstruction efficiency

Results of Inclusive Fiducial Cross Section

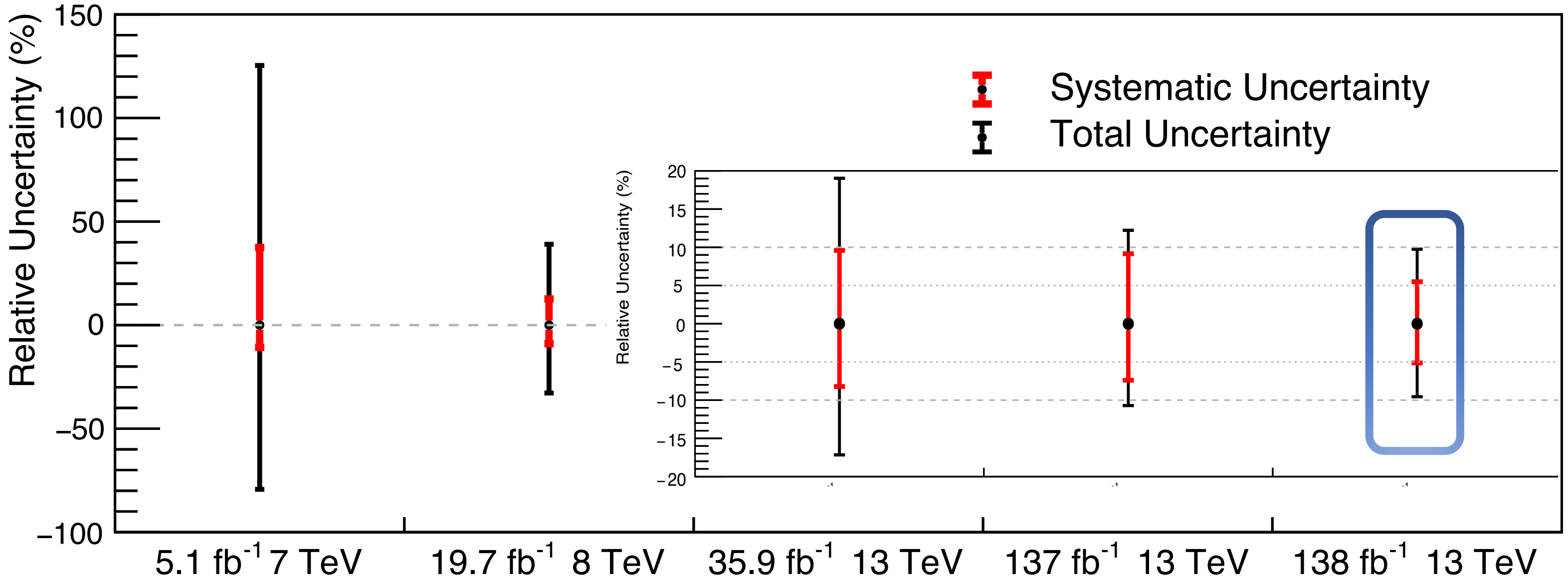

JHEP04(2016)005 JHEP04(2016)005 JHEP11(2017)047 EPJC81(2021)488 CMS-PAS-HIG-21-009

10% precision

$$\sigma^{\text{fid}} = 2.73^{+0.22}_{-0.22}\,(\text{stat})^{+0.15}_{-0.14}\,(\text{syst})\,\text{fb}$$
$$= 2.73^{+0.22}_{-0.22}\,(\text{stat})^{+0.12}_{-0.12}(\text{electrons})^{+0.06}_{-0.05}(\text{lumi})^{+0.04}_{-0.04}(\text{bkg})^{+0.03}_{-0.02}(\text{muons})\,\text{fb}$$

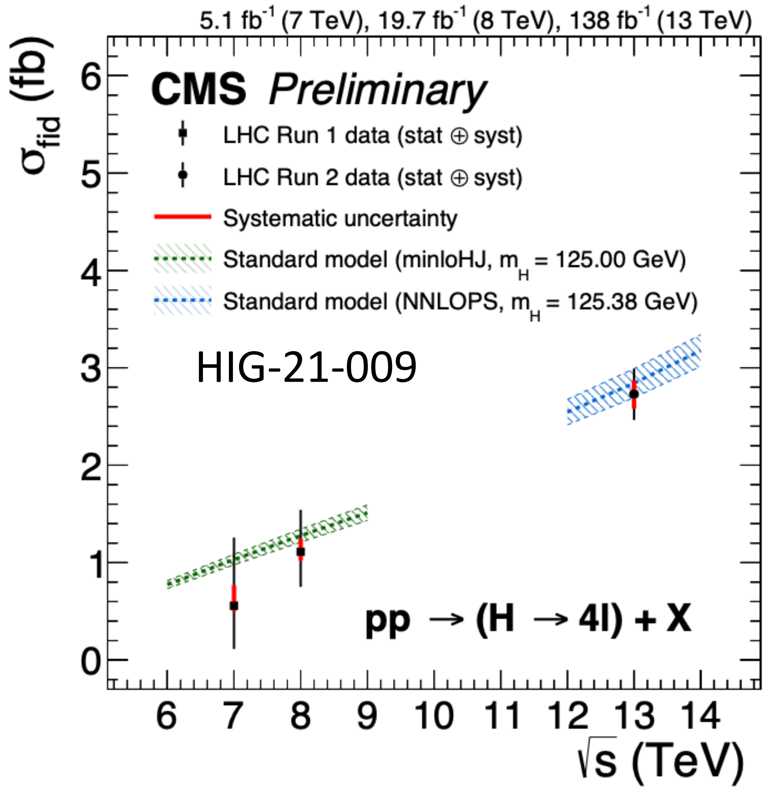

Fiducial cross section as a function of center of mass

- Systematic uncertainty dominated by
  - Electrons-related nuisances,
  - Especially electron reconstruction efficiency
- **Reduction of the systematic component** due to the reduction of the main lepton nuisances

Differential Fiducial Cross Section

- Higgs **production** observables (12):

$$\boldsymbol{p_T^H} \quad \boldsymbol{|y_H|} \quad \boldsymbol{N_{jets}} \quad \boldsymbol{p_T^{j1}}$$
$$p_T^{j2} \quad m_{jj} \quad |\Delta\eta_{jj}|$$
$$p_T^{Hj} \quad m_{Hj} \quad p_T^{Hjj} \quad \mathcal{T}_B \quad \mathcal{T}_C$$

- Higgs **decay** observables (13):

$$m_{Z1} \quad m_{Z2} \quad \Phi \quad \Phi_1 \quad \cos\theta \quad \cos\theta_1 \quad \cos\theta^*$$
$$\mathcal{D}_{0-}^{\mathrm{dec}} \quad \mathcal{D}_{cp}^{\mathrm{dec}} \quad \mathcal{D}_{0h+}^{\mathrm{dec}} \quad \mathcal{D}_{\Lambda1}^{\mathrm{dec}} \quad \mathcal{D}_{\Lambda1}^{Z\gamma,\mathrm{dec}} \quad \mathcal{D}_{int}^{\mathrm{dec}}$$

- **Double** differential observables (6):

m_{Z1} vs m_{Z2} $\quad$ N_{jets} vs p_T^H

p_T^{j1} vs p_T^{j2} $\quad$ $\mathcal{T}_C$ vs p_T^H

p_T^{Hj} vs p_T^H $\quad$ $|y^H|$ vs p_T^H

1D Differential Cross Section --- Production

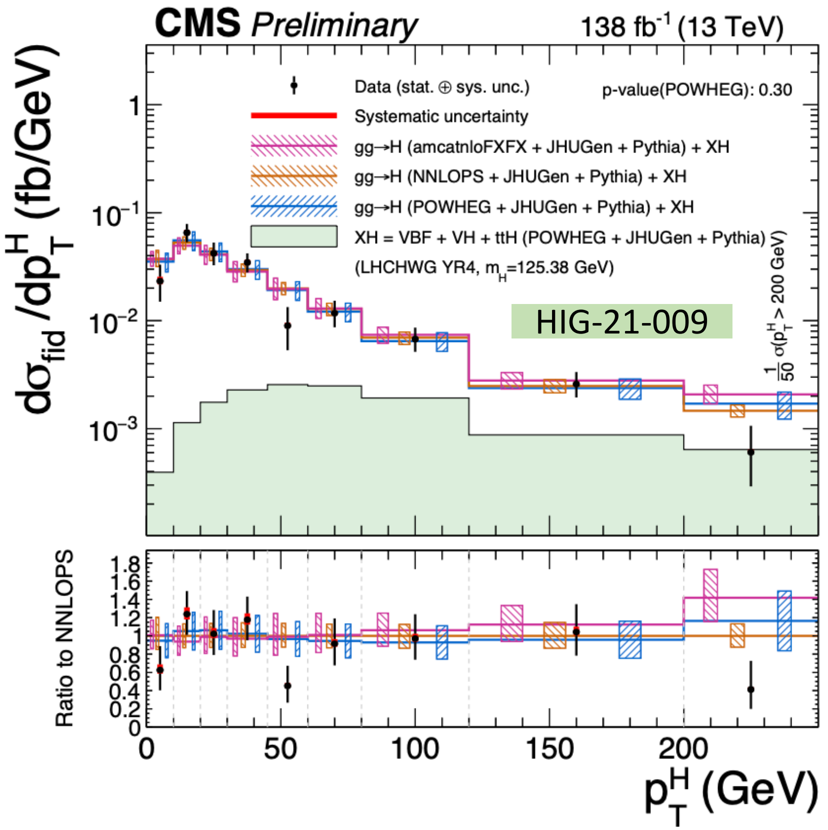

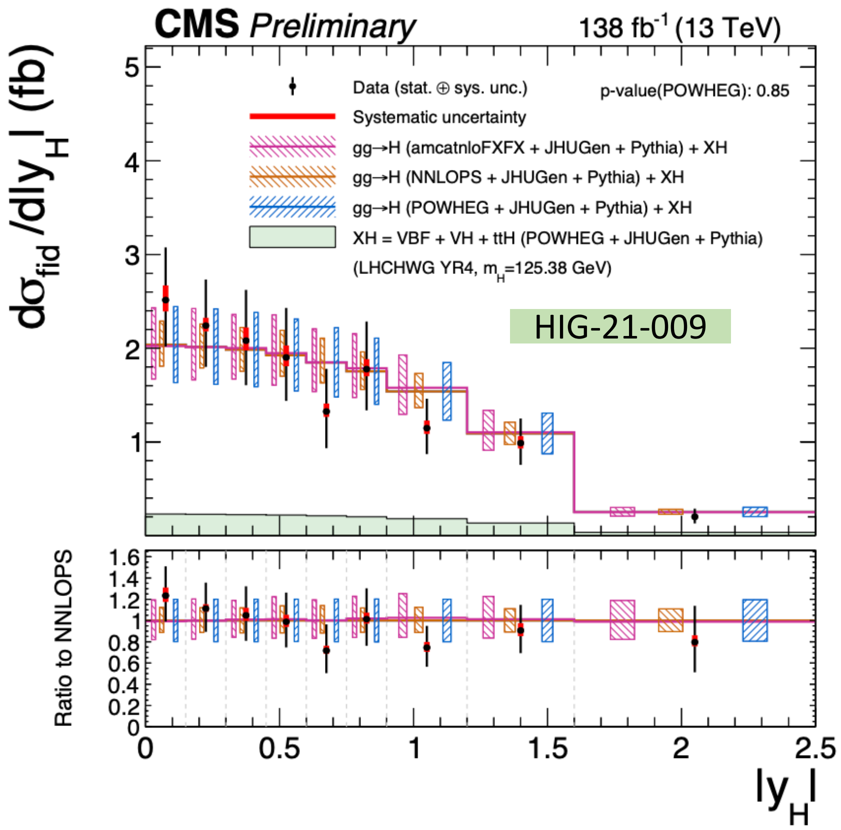

- Differential observables of **Higgs boson kinematics**
  - P_T^H: probes the perturbative QCD modelling of this production mechanism
  - $|y^H|$: sensitive to the gluon fusion production mechanism and PDFs
- Average precision of 35%

1D Differential Cross Section --- Production

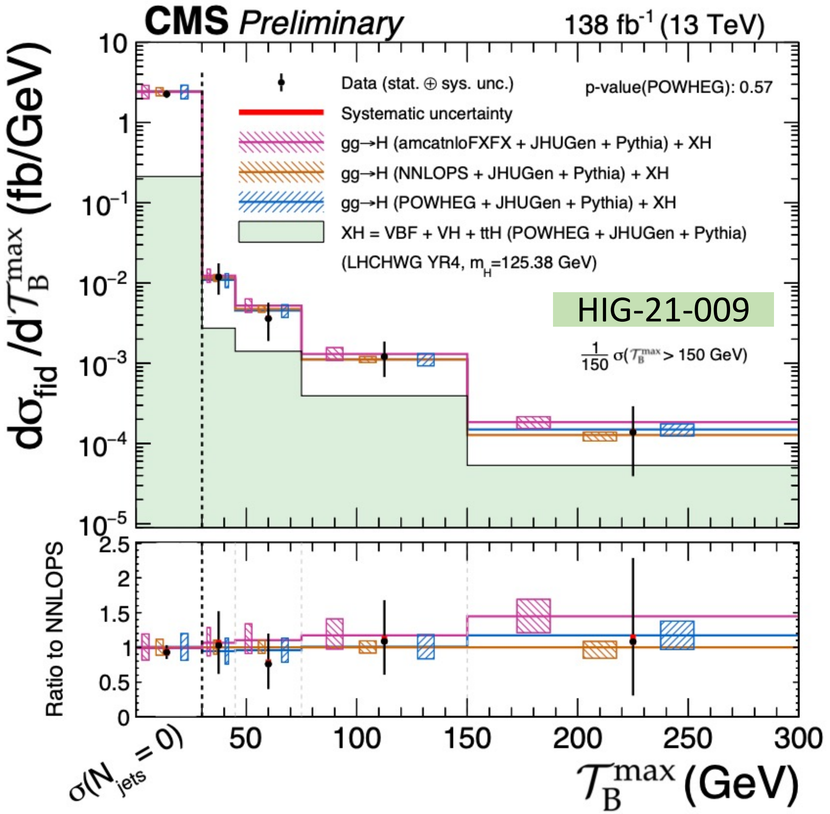

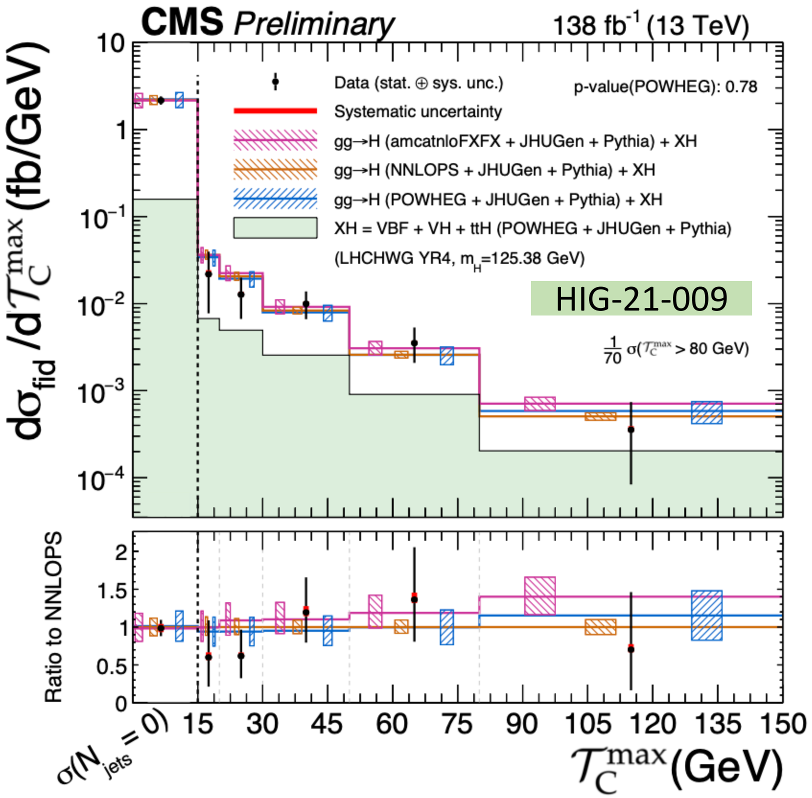

- Differential observables of **Jet activity**
  - Jet rapidity-weighted observables $\mathcal{T}_B^{max} = \max_j(m_T^j e^{-|y_j - y_H|})$ $\mathcal{T}_C^{max} = \max_j(\frac{\sqrt{E_j^2 - p_{z,j}^2}}{2\cosh(y_j - y_H)})$
  - Maximum is taken among all jets and events with $\mathcal{T}_B \leq 30$ GeV and $\mathcal{T}_C \leq 15$ GeV make the 0-jet bin
  - The advantage of such observables is that they can be ***factorized and resumed*** allowing for ***precise theory predictions***.

1D Differential Cross Section --- Decay

- Higgs **Decay** in 4l final states could be characterized by the following seven parameters:
  - m_{Z1}, m_{Z2}
  - Φ , Φ_1 , $\cos\theta$, $\cos\theta_1$, $\cos\theta^*$

☆ $\mathcal{D}^{dec}_{0-}$ $\mathcal{D}^{dec}_{cp}$ | $\mathcal{D}^{dec}_{0h+}$ $\mathcal{D}^{dec}_{int}$ | $\mathcal{D}^{dec}_{\Lambda1}$ $\mathcal{D}^{Z\gamma,dec}_{\Lambda1}$

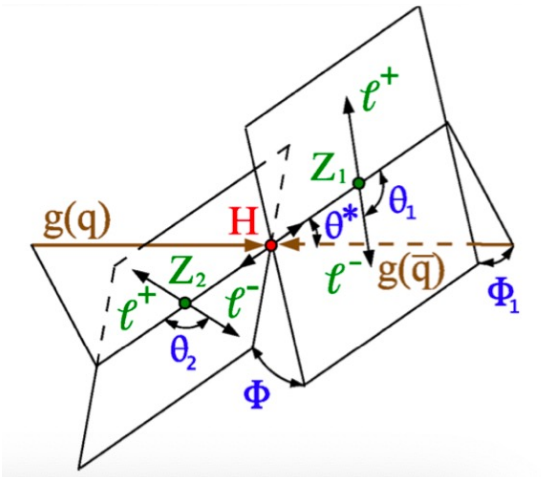

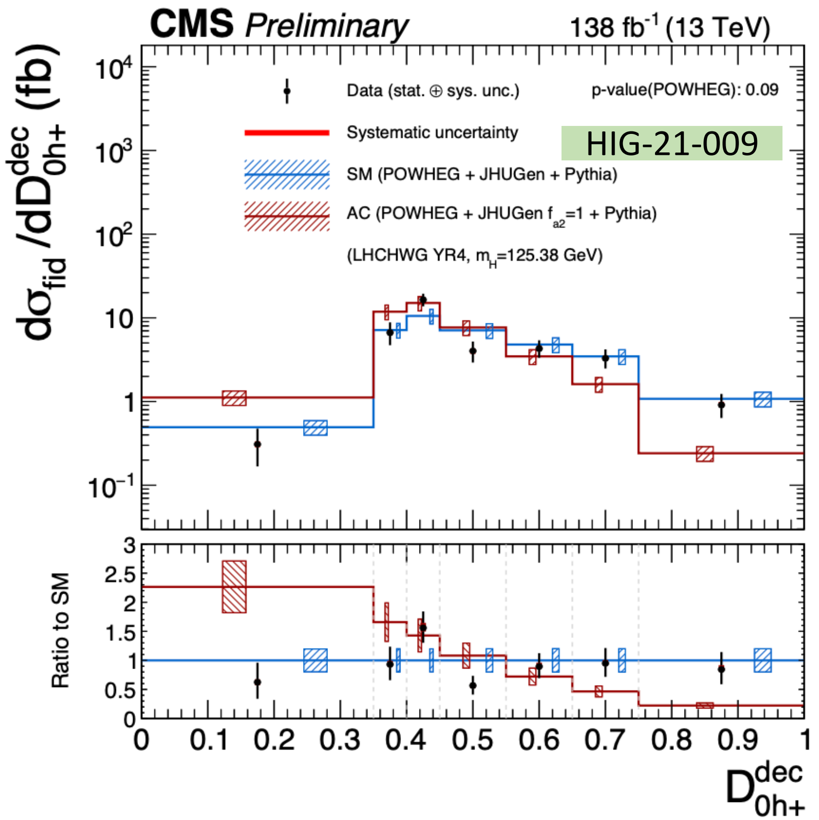

- Higher order spin-zero 0_h^+ a_2:
  sensitive to possible BSM contributions from heavy H bosons

- 13 Differential cross sections of decay are also measured in the **same-flavor** and **different flavor** final states.
- Its final state is sensitive to ***interference effects***

1D Differential Cross Section --- Decay

- Higgs **Decay** in 4l final states could be characterized by the following seven parameters:
  - $m_{Z1},\ m_{Z2}$
  - $\Phi\ ,\ \Phi_1\ ,\ \cos\theta\ ,\ \cos\theta_1\ ,\ \cos\theta^*$

☆ $\mathcal{D}^{dec}_{0-}$ $\mathcal{D}^{dec}_{cp}$ | $\mathcal{D}^{dec}_{0h+}$ $\mathcal{D}^{dec}_{int}$ | $\mathcal{D}^{dec}_{\Lambda1}$ $\mathcal{D}^{Z\gamma,dec}_{\Lambda1}$

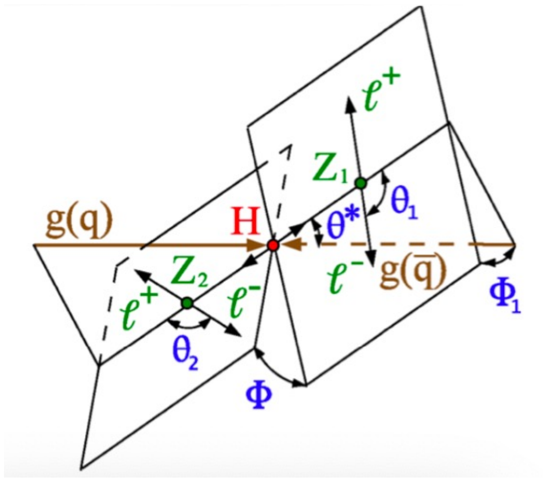

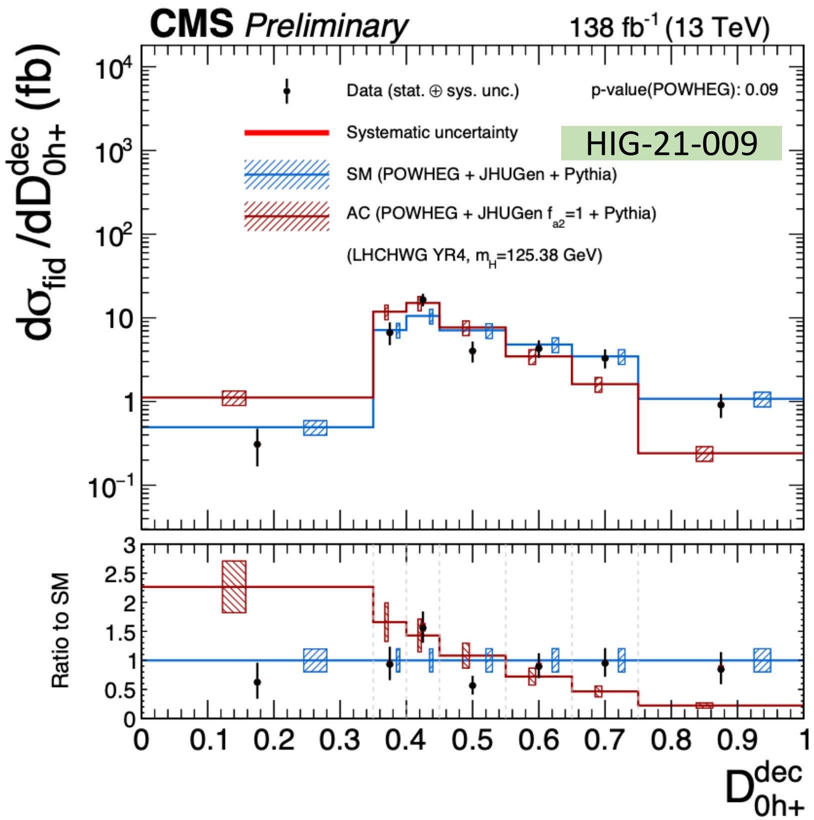

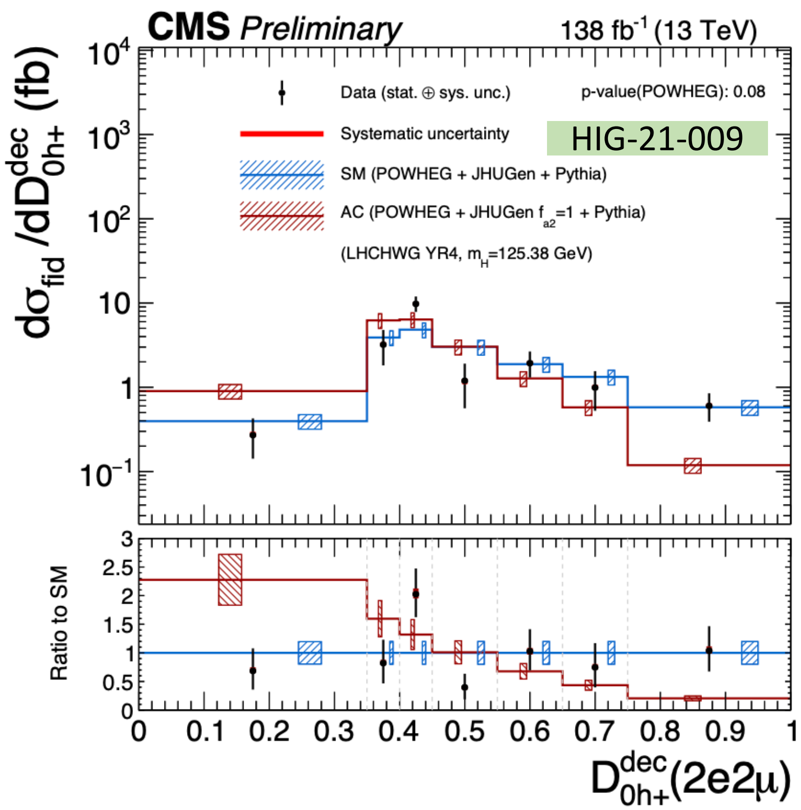

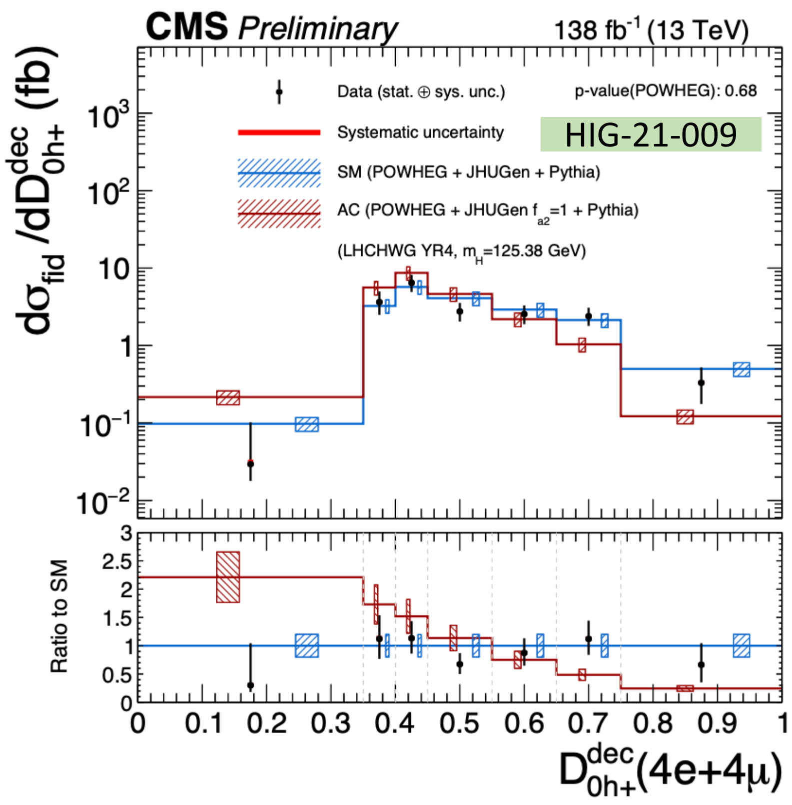

Constraints on the H boson self-coupling

Probing κ_λ via single-Higgs decay

- Differential XS measurement as a function of p_T^H ⇨ extract limits on H boson self coupling.

production decay

$$\mu_i^f = \mu_i \times \mu^f = \frac{\sigma^{NLO}}{\sigma^{NLO}_{SM}} \frac{BR(H\to ZZ)}{BR^{SM}(H\to ZZ)} = \frac{1+\kappa_\lambda C_{1,i}+\delta Z_H}{(1-(\kappa_\lambda^2-1)\delta Z_H)(1+C_{1,i}+\delta Z_H)} \times \left[1+\frac{(\kappa_\lambda-1)(C_1^{\Gamma ZZ}-C_1^{\Gamma tot})}{1+(\kappa_\lambda-1)C_1^{\Gamma tot}}\right]$$

- Cross sections of different production mechanisms of H boson is parameterized as a function of

$$\kappa_\lambda = \lambda_3/\lambda_3^{SM}$$

- The corresponding observed (expected) excluded κ_λ range at 95% CL

$$-5.5(-7.7) < \kappa_\lambda < 15.1(17.9)$$

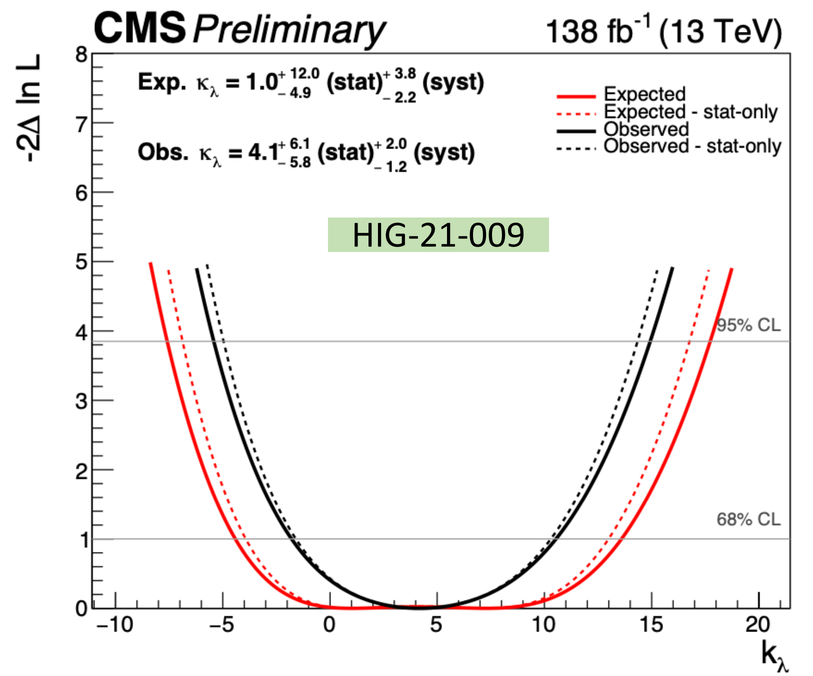

Constraints on Higgs boson couplings modifier

Probing κ_b, κ_c via p_T^H differential cross section

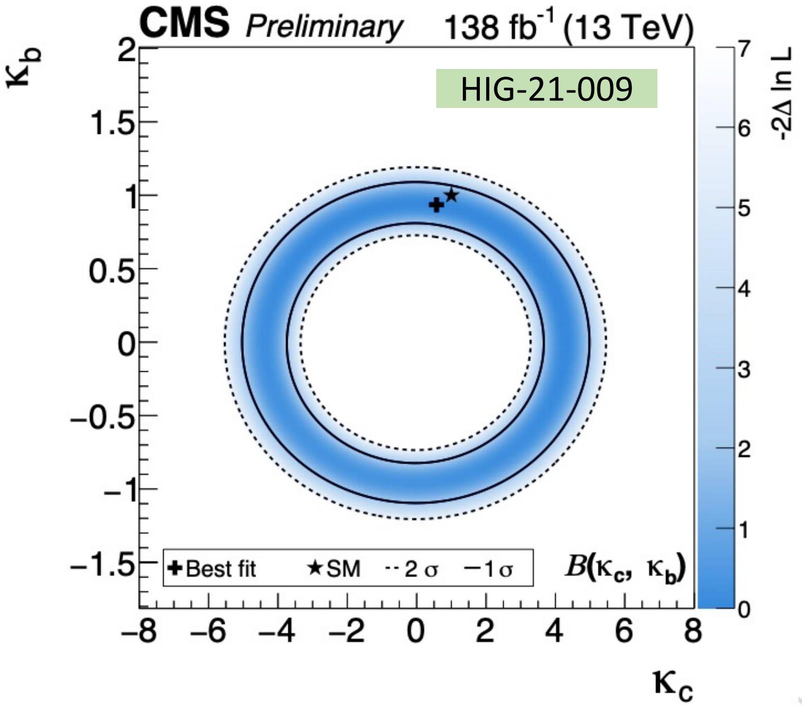

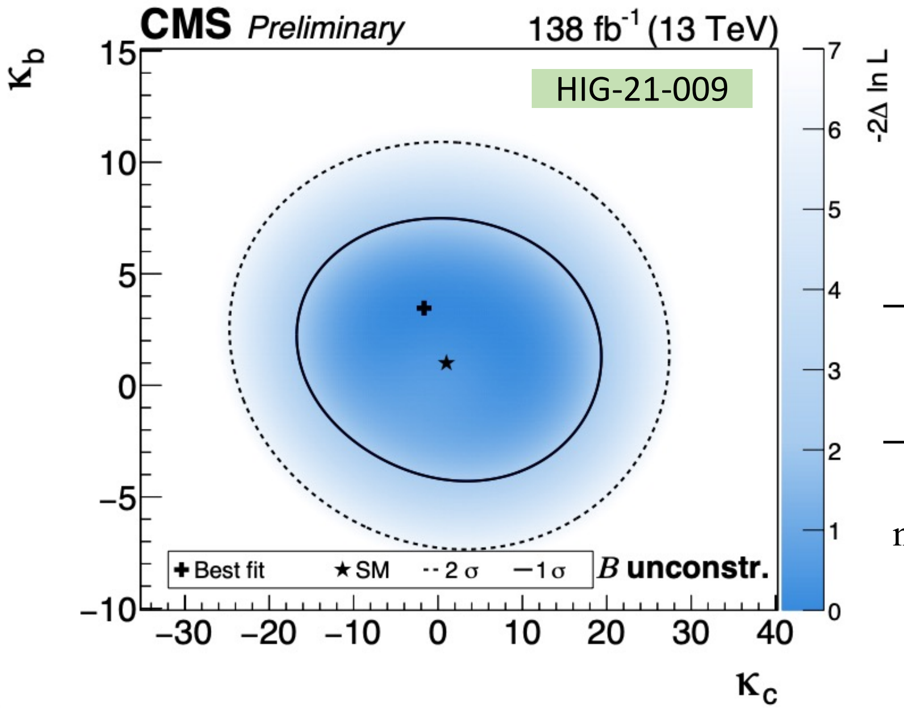

HIG-21-009		Full Run2 Ultra Legacy Floating κ_b κ_c	
		Observed 95% confidence interval	**Expected** 95% confidence interval
Shape-Only	κ_b	[-5.6, 8.9]	[-5.5, 7.4]
	κ_c	[-20, 23]	[-19, 20]
Shape+ normalization	κ_b	[-1.1, 1.1]	[-1.3, 1.2]
	κ_c	[-5.3, 5.2]	[-5.7, 5.7]

- Simultaneous fit for coupling modifier κ_b, κ_c assuming
  - (left) coupling dependence of the branching fractions (*shape+normalization*)
  - (right)branching fractions implemented as nuisance parameters with no prior constraint (*shape-only*)
- Observed and expected 95% confidence intervals for the Yukawa coupling modifiers

Summary

- Measurements of Higgs boson cross section in four-lepton final state at $\sqrt{s} = 13TeV$ using data sample corresponding to an integrated luminosity of 138 fb^{-1}.
  - The **inclusive fiducial cross section** measured is $\sigma^{fid} = 2.73^{+0.22}_{-0.22}(stat.)^{+0.15}_{-0.14}(sys.)$ fb.
  - **Differential** cross sections as a function of **31 observables** are measured, including one and **two dimension observables**, which involves the
    - H boson production and **HZZ decay**, jet related observables, and observables sensitive to spin and CP quantum numbers
    - Complete coverage of the whole phase space
  - The measurement of fiducial cross section in bins of the transverse momentum is reinterpreted to set constraints to
    - **H boson self-coupling** (κ_λ)
    - **Couplings to bottom and charm quarks** (κ_b, κ_c)
- All results are consistent, within their uncertainties, with the expectations for the Standard Model H boson.


Thanks for your attention!

Backup

Fiducial/Differential Cross Section of 4l

- Definition of the fiducial phase space of $H \rightarrow ZZ \rightarrow 4l$
- Number of events of different final state *f* and different year *y* in the given bin *i* are expressed as a function of 4l invariable mass

HIG-21-009

Requirements for the $H \to ZZ \to 4\ell$ fiducial phase space	
Lepton kinematics and isolation	
Leading lepton p_T	$p_T > 20\,\text{GeV}$
Sub-leading lepton p_T	$p_T > 10\,\text{GeV}$
Additional electrons (muons) p_T	$p_T > 7(5)\,\text{GeV}$
Pseudorapidity of electrons (muons)	$\lvert\eta\rvert < 2.5\ (2.4)$
Sum of scalar p_T of all stable particles within $\Delta R < 0.3$ from lepton	$< 0.35 p_T$
Event topology	
Existence of at least two same-flavor OS lepton pairs, where leptons satisfy criteria above	
Inv. mass of the Z_1 candidate	$40 < m_{Z_1} < 120\,\text{GeV}$
Inv. mass of the Z_2 candidate	$12 < m_{Z_2} < 120\,\text{GeV}$
Distance between selected four leptons	$\Delta R(\ell_i, \ell_j) > 0.02$ for any $i \neq j$
Inv. mass of any opposite sign lepton pair	$m_{\ell^+\ell'^-} > 4\,\text{GeV}$
Inv. mass of the selected four leptons	$105 < m_{4\ell} < 160\,\text{GeV}$

$$N^{f,i,y}_{\text{obs}}(m_{4\ell}) = N^{f,i,y}_{\text{fid}}(m_{4\ell}) + N^{f,i,y}_{\text{nonfid}}(m_{4\ell}) + N^{f,i,y}_{\text{nonres}}(m_{4\ell}) + N^{f,i,y}_{\text{bkg}}(m_{4\ell})$$
$$= \sum_{j}^{\text{genBin}} \epsilon^{f,y}_{i,j,y} \cdot (1 + f^{f,i,y}_{\text{nonfid}}) \cdot \sigma^{f,j,y}_{\text{fid}} \cdot \mathcal{L} \cdot \mathcal{P}^{f,y}_{\text{res}}(m_{4\ell})$$
$$+ N^{f,i,y}_{\text{nonres}} \cdot \mathcal{P}^{f,y}_{\text{nonres}}(m_{4\ell}) + N^{f,i,y}_{\text{bkg}} \cdot \mathcal{P}^{f,i,y}_{\text{bkg}}(m_{4\ell})$$

HIG-21-009

- Fiducial + non-fiducial resonances signal contribution:
  - Shape is described by double-sided Crystal Ball function.
  - Normalization is proportional to the fiducial cross section.
- Non-resonant signal contribution
  - Arises from WH, ZH ttH where one of the leptons from Higgs is lost or not selected.
  - Modeled by Landau distribution
  - Treated as background

OBJECTS

• Electrons

- Loose electrons
  - $P_T > 7$GeV; $|\eta| < 2.5$
  - $d_{xy} < 0.5\ cm;\ d_z < 1\ cm;\ SIP_{3D} < 4$
- BDT cut based on ID+Iso in 6 ($|\eta|$, P_T)bins

• Muons

- Loose muons
  - $P_T > 5$GeV; $|\eta| < 2.4$
  - $d_{xy} < 0.5\ cm;\ d_z < 1\ cm;\ SIP_{3D} < 4$
- PF muon ID if $P_T < 200$ GeV, PF muon ID or High-pT muon ID if $P_T > 200$ GeV,
- RelPFIso($\Delta R = 0.3$) < 0.35

$$\mathcal{I}^{\ell} \equiv \left(\sum p_{\mathrm{T}}^{\mathrm{charged}} + \max\left[0, \sum p_{\mathrm{T}}^{\mathrm{neutral}} + \sum p_{\mathrm{T}}^{\gamma} - p_{\mathrm{T}}^{\mathrm{PU}}(\ell)\right] \right) / p_{\mathrm{T}}^{\ell}$$

$$\Delta R(i,j) = \sqrt{(\eta^i - \eta^j)^2 + (\phi^i - \phi^j)^2}$$

• FSR photon

- $P_{T,\gamma} > 2$ GeV;$|\eta^{\gamma}| < 2.4$;relPFIso<1.8
- Associated γ to the closest loose lepton
- $\Delta R(\gamma, l) < 0.5$; $\frac{\Delta R(\gamma,l)}{E_{T,\gamma}^2} < 0.012$; choose photon with lowest $\frac{\Delta R(\gamma,l)}{E_{T,\gamma}^2}$
- Remove selected FSRs from lepton isolation cone for all loose leptons

• Jets

- AK4 PFCHs jets
- $P_T > 30$ GeV; $|\eta| < 4.7$; Tight PF jet ID
- Cleaned $\Delta R(jet, l/\gamma) > 0.4$
- Cut-based jet ID (tight WP); Jet pileup ID (tight WP)

HIG-21-009

Event reconstruction and selections

- Loose e (μ) passing selections $p_T > 7(5)$GeV; $|\eta| < 2.5(2.4)$; vertex cut $d_{xy} < 0.5\ cm$; $d_z < 1\ cm$;$SIP_{3D} < 3$; Tight Selections based on BDT method for e (PF μ RelPFIso< 0.35);
- Z candidate
  - Any OS-SF pair that satisfy $12 < m_{ll(\gamma)} < 120$ GeV
- Build all possible ZZ candidates defined as pairs of non-overlapping Z candidate; define Z_1 candidate with $m_{ll(\gamma)}$ closest to the POG m(Z) mass
  - $m_{Z1} > 40$ GeV; $p_T(l1) > 20$ GeV; $p_T(l2) > 10$ GeV
  - $\Delta R > 0.02$ between each of the four leptons
  - $m_{ll} > 4$ GeV for OS pairs (regardless of flavour)
  - Reject 4μ and 4e candidates where the alternative pair Z_aZ_b satisfies $|m_{Z_a} - m_Z| < |m_{Z_1} - m_Z|$ and $m_{Z_b} < 12$ GeV
  - $m_{4l} > 70$ GeV
- If more than one ZZ candidate is left, take the one with Z_1 mass closest to m_Z and the Z_2 from the candidates whose lepton give higher p_T sum

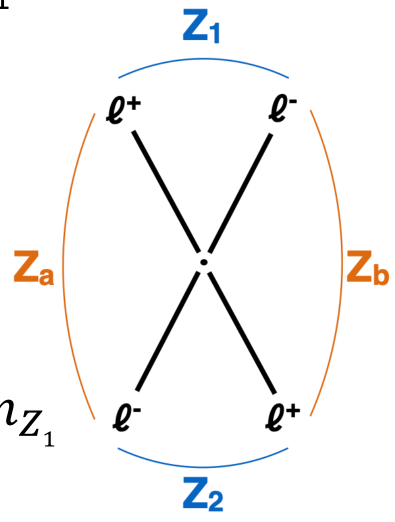

Background estimation

- Irreducible background
  - $q\bar{q} \to ZZ$
  - $gg \to ZZ$
  - Estimated using simulation

- Reducible background
  - Misidentified leptons
  - Secondary produced leptons
  - Two independent methods used to estimated Z+X background: OS and SS
    - Fake rates calculated in Z+l control region
    - Z+X yields estimated in orthogonal regions of Z+ll control region
    - Final estimate combination of 2 methods
  - Templates are built from the control regions in data

Background normalization

---- **only** applied in **inclusive** cross section measurement due to statistics

- In previous HIG-19-001, ZZ background from MC predictions
  - Both shape and normalization
  - Mass4l [105, 140]
- Several studies carried out to assess the measurement’s precision
  - Its ZZ normalization from data sidebands
  - Improvement of estimation as well as **reduction in uncertainties**
    - because luminosity and other theoretical uncertainties no longer contribute to the normalization.

ZZ floating approach:

--- inclusive normalization for qqZZ and ggZZ process profiled in the fit

Systematics Uncertainties

- Experimental uncertainties
  - Integrated luminosity
  - Lepton identification and reconstruction efficiency
  - Reducible background
  - Lepton scale and resolution
  - Jet energy scale
- Theoretical uncertainties
  - **QCD uncertainty**
  - Uncertainty on the Choice of **PDF set**
  - Uncertainty of 2% on H → 4l **branching ratio**

The uncertainties of lepton reconstruction and selection range for
- 4μ channel 0.6 - 1.9%
- 4e channel 4.3 – 10.9%

A reduction in the 4e uncertainties thanks to a dedicated RMS method.

HIG-21-009	Common experimental uncertainties		
	2016	2017	2018
Luminosity uncorrelated	1 %	2 %	1.5 %
Luminosity corr 16 17 18	0.6 %	0.9 %	2 %
Luminosity corr 17 18	-	0.6 %	0.2 %
Lepton id/reco efficiencies	0.7–10 %	0.6 – 8.5 %	0.6 – 9.5 %
	Background related uncertainties		
Reducible background (Z+X)	25 – 43 %	23 – 36 %	24 –36 %
	Signal related uncertainties		
Lepton energy scale	0.01%(μ) - 0.06%(e)	0.01%(μ) - 0.06%(e)	0.01%(μ) - 0.06%(e)
Lepton energy resolution	3%(μ) - 10%(e)	3%(μ) - 10%(e)	3%(μ) - 10%(e)

Distribution of p_T^H and $|y_H|$

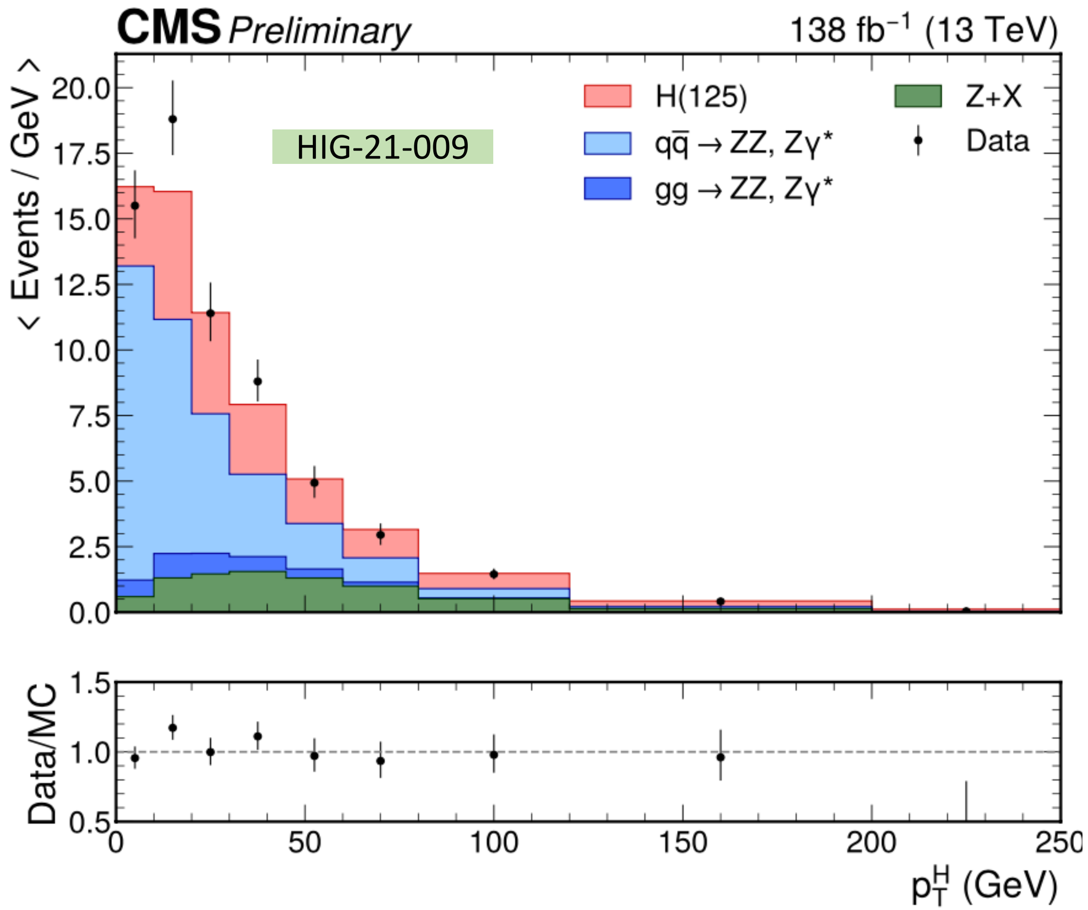

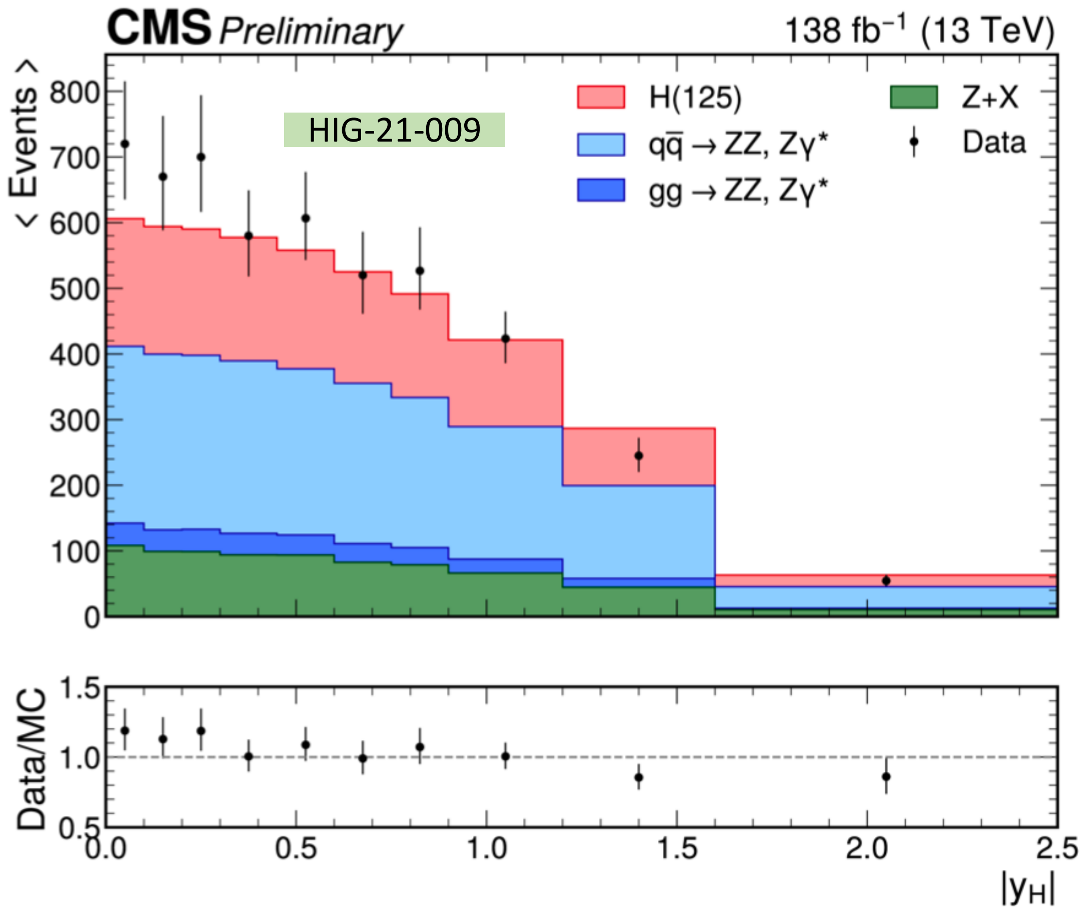

- Points with error bars represent the data, while the solid histograms represent the MC simulation.

Fiducial/Differential Cross Section

- An alternative approach to study the properties of the Higgs boson
- Cross section of bin i is defined as:

$$\sigma_i = \frac{N_{reco,i}}{C_i * A_i * L * B}$$

- **Fiducial cross section** = cross section in fiducial volume (cuts applied to generated events)

$$\sigma_{fid,i} * B = \frac{N_{reco,i}}{C_i * L}$$

- **Higgs boson kinematics**:
  - P_T^H: probes the perturbative QCD modelling of this production mechanism
  - $|\eta^H|$: sensitive to the gluon fusion production mechanism and PDFs
- **Jet activity:** N_{jets}; P_T and η of leading (sub) jet; $\mathcal{T}_B, \mathcal{T}_C$ …
  - sensitive to the theoretical modelling and relative Higgs production.
- **Spin and CP quantum numbers:** Angular observables, such as $\Phi, \Phi_1, \cos\theta_1, \cos\theta_2$, $|cos\theta^*|$:
  - sensitive to the spin and charge conjugation and parity properties of the Higgs
- **Higgs boson production mechanisms**
  - specific fiducial regions may be constructed

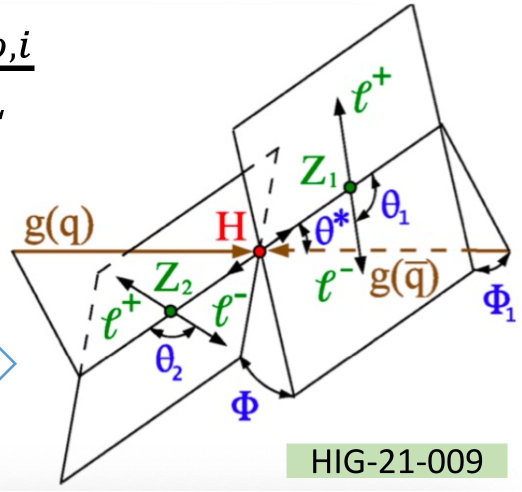

Results of Measurements

Inclusive fiducial cross section

Irreducible background normalization taken from MC simulation and ZZ floating in the fit

Interpretations

k_λ, k_b, k_c

Differential observables Higgs Production

p_T^H $|y_H|$

N_{jets} p_T^{j1} p_T^{j2} m_{jj} $|\boldsymbol{\Delta\eta_{jj}}|$

p_T^{Hj} m_{Hj} p_T^{Hjj} $\mathcal{T}_B$ $\mathcal{T}_C$

Differential observables Higgs decay

m_{Z1} m_{Z2}

Φ Φ_1 $\cos\theta$ $\cos\theta_1$ $\cos\theta^*$

$\mathcal{D}_{0-}^{\text{dec}}$ $\mathcal{D}_{cp}^{\text{dec}}$ $\mathcal{D}_{0h+}^{\text{dec}}$ $\mathcal{D}_{\Lambda1}^{\text{dec}}$ $\mathcal{D}_{\Lambda1}^{Z\gamma,\text{dec}}$ $\mathcal{D}_{int}^{\text{dec}}$

Double differential observables

m_{Z1} vs m_{Z2} N_{jets} vs p_T^H

$\mathcal{T}_C$ vs p_T^H $|y^H|$ vs p_T^H

p_T^{Hj} vs p_T^H p_T^{j1} vs p_T^{j2}

Results of measurements

Inclusive fiducial cross section

Irreducible background normalization taken from MC simulation and ZZ floating in the fit

Interpretations

k_λ, k_b, k_c

Differential observables Higgs Production

p_T^H $|y_H|$

N_{jets} p_T^{j1} p_T^{j2} m_{jj} $|\boldsymbol{\Delta\eta_{jj}}|$

p_T^{Hj} m_{Hj} p_T^{Hjj} $\mathcal{T}_B$ $\mathcal{T}_C$

Differential observables Higgs decay

m_{Z1} m_{Z2}

Φ Φ_1 $\cos\theta$ $\cos\theta_1$ $\cos\theta^*$

$\mathcal{D}_{0-}^{\mathrm{dec}}$ $\mathcal{D}_{cp}^{\mathrm{dec}}$ $\mathcal{D}_{0h+}^{\mathrm{dec}}$ $\mathcal{D}_{\Lambda1}^{\mathrm{dec}}$ $\mathcal{D}_{\Lambda1}^{Z\gamma,\mathrm{dec}}$ $\mathcal{D}_{int}^{\mathrm{dec}}$

Double differential observables

m_{Z1} vs m_{Z2} N_{jets} vs p_T^H

$\mathcal{T}_C$ vs p_T^H $|y^H|$ vs p_T^H

p_T^{Hj} vs p_T^H p_T^{j1} vs p_T^{j2}

Results of Inclusive Fiducial Cross Section

- The integrated fiducial cross section for $H \rightarrow ZZ \rightarrow 4l$ process is measured to be

HIG-21-009

$$\sigma^{\text{fid}} = 2.73^{+0.22}_{-0.22}\,(\text{stat})^{+0.15}_{-0.14}\,(\text{syst})\,\text{fb}$$
$$= 2.73^{+0.22}_{-0.22}\,(\text{stat})^{+0.12}_{-0.12}(\text{electrons})^{+0.06}_{-0.05}(\text{lumi})^{+0.04}_{-0.04}(\text{bkg})^{+0.03}_{-0.02}(\text{muons})\,\text{fb}$$

in good agreement with the SM expectation.

- The systematic uncertainty dominated by
  - Electrons-related nuisances,
    - Especially electron reconstruction efficiency

HIG-21-009

Signal process	$\mathcal{A}_{\text{fid}}$	ϵ	f_{nonfid}	$(1+f_{\text{nonfid}})\epsilon$
ggH (POWHEG)	0.408 ± 0.001	0.619 ± 0.001	0.053 ± 0.001	0.652 ± 0.001
VBF	0.448 ± 0.001	0.632 ± 0.002	0.043 ± 0.001	0.659 ± 0.002
WH	0.332 ± 0.001	0.616 ± 0.002	0.077 ± 0.001	0.664 ± 0.002
ZH	0.344 ± 0.002	0.626 ± 0.003	0.083 ± 0.002	0.678 ± 0.003
$t\bar{t}H$	0.320 ± 0.002	0.614 ± 0.003	0.179 ± 0.003	0.725 ± 0.005

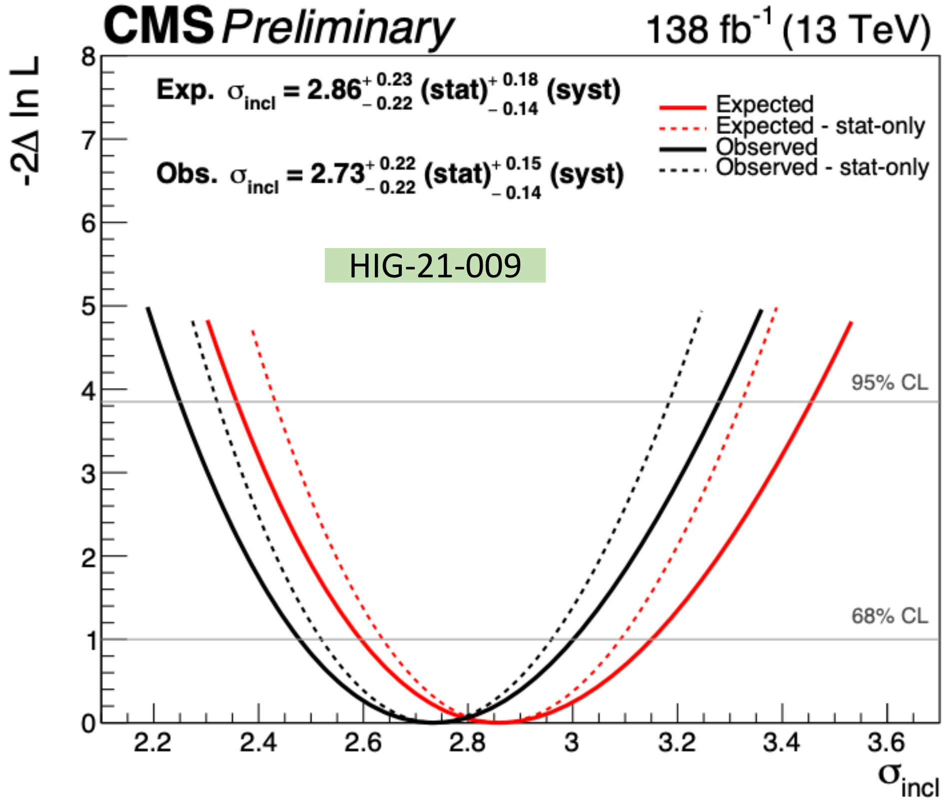

Results of Inclusive Fiducial Cross Section

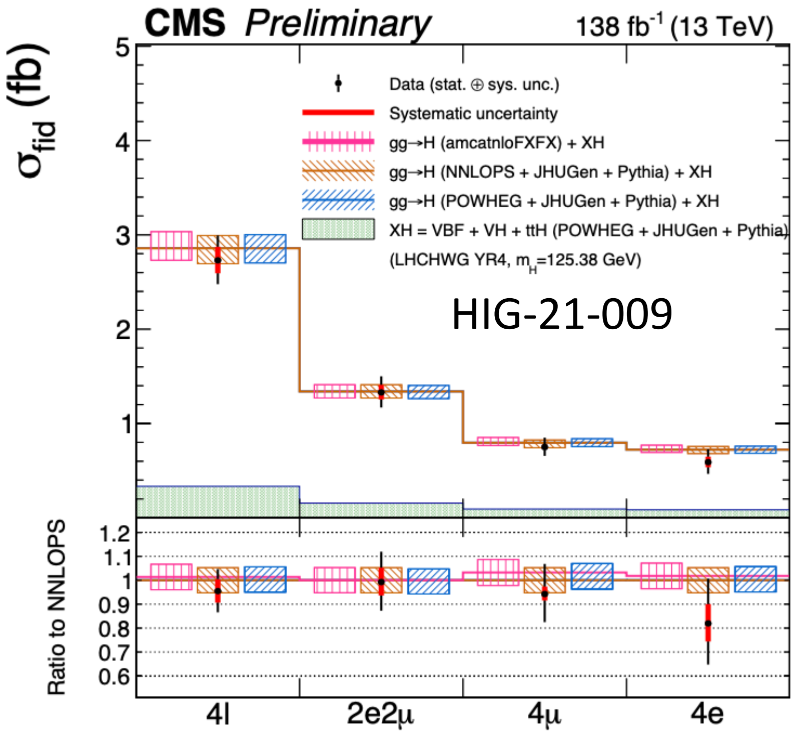

$$\sigma^{fid} = 2.73^{+0.22}_{-0.22}(\mathrm{stat})^{+0.15}_{-0.14}(\mathrm{sys})\mathrm{fb}$$

Irreducible background normalization taken from MC simulation

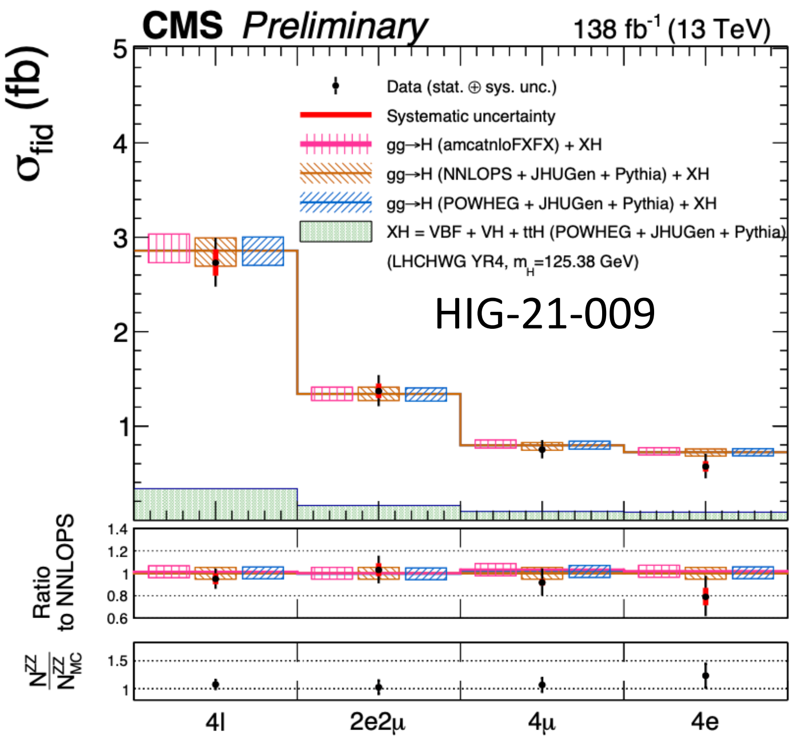

$$\sigma^{fid} = 2.74^{+0.24}_{-0.23}(\mathrm{stat})^{+0.14}_{-0.11}(\mathrm{sys})\mathrm{fb}$$

Irreducible background normalization ZZ floating in the fit

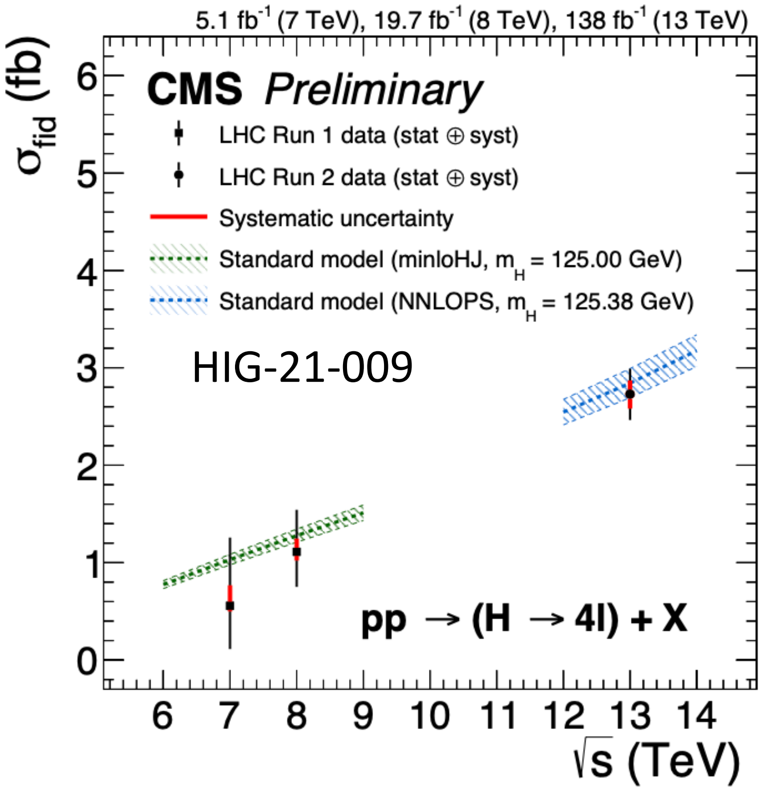

Fiducial cross section as a function of center of mass

- Remove the impact of nuisances on ZZ normalization
- Being sensitive to BSM effects in the background

Results of measurements

Inclusive fiducial cross section

Irreducible background normalization taken from MC simulation and ZZ floating in the fit

Interpretations

k_λ, k_b, k_c

Differential observables Higgs Production

p_T^H $|y_H|$

N_{jets} p_T^{j1} p_T^{j2} m_{jj} $|\Delta\eta_{jj}|$

p_T^{Hj} m_{Hj} p_T^{Hjj} $\mathcal{T}_B$ $\mathcal{T}_C$

Differential observables Higgs decay

m_{Z1} m_{Z2}

Φ Φ_1 $\cos\theta$ $\cos\theta_1$ $\cos\theta^*$

$\mathcal{D}_{0-}^{\text{dec}}$ $\mathcal{D}_{cp}^{\text{dec}}$ $\mathcal{D}_{0h+}^{\text{dec}}$ $\mathcal{D}_{\Lambda1}^{\text{dec}}$ $\mathcal{D}_{\Lambda1}^{Z\gamma,\text{dec}}$ $\mathcal{D}_{int}^{\text{dec}}$

Double differential observables

m_{Z1} vs m_{Z2} N_{jets} vs p_T^H

$\mathcal{T}_C$ vs p_T^H $|y^H|$ vs p_T^H

p_T^{Hj} vs p_T^H p_T^{j1} vs p_T^{j2}

1D Differential Cross Section --- Production

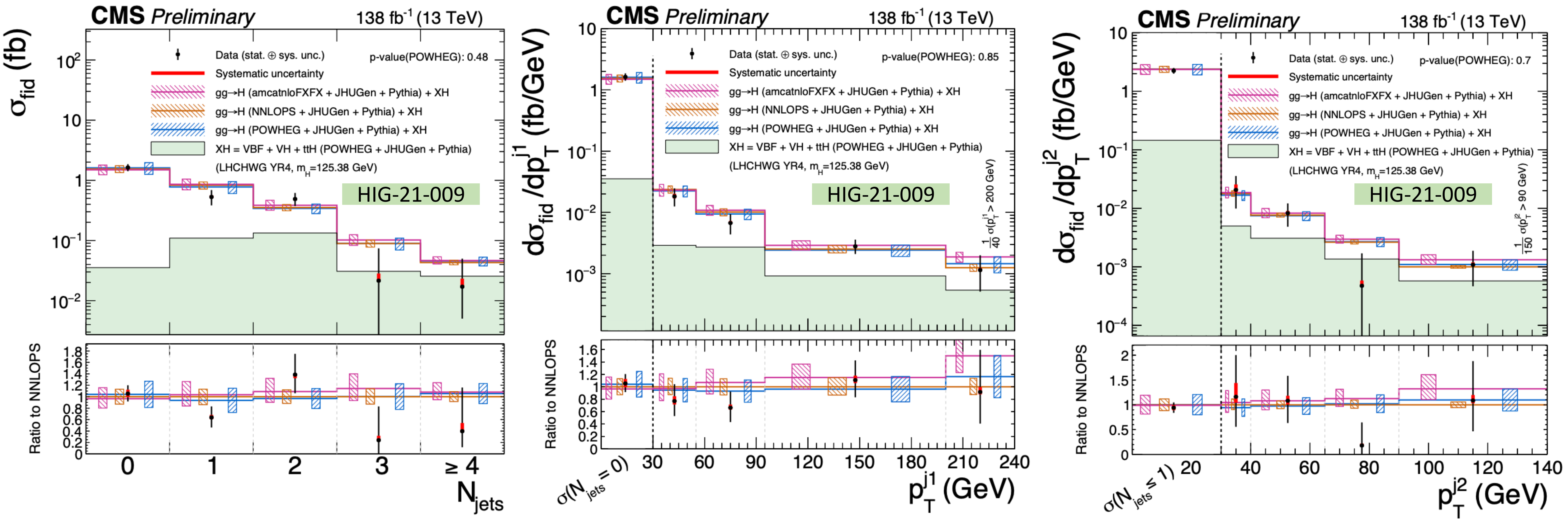

- Differential observables of **Jet activity**
  - Number of the associated jets
  - Transverse momentum of leading jet and subleading jet
  - sensitive to the theoretical modelling and relative Higgs production.

1D Differential Cross Section --- Production

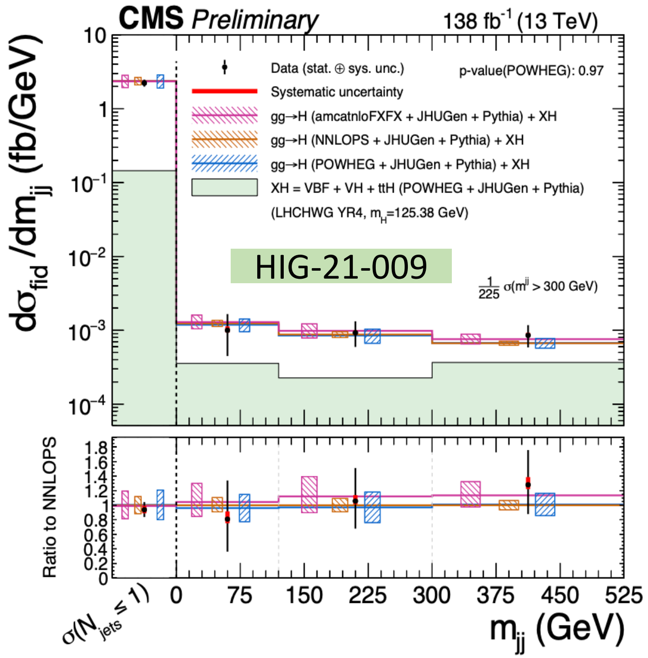

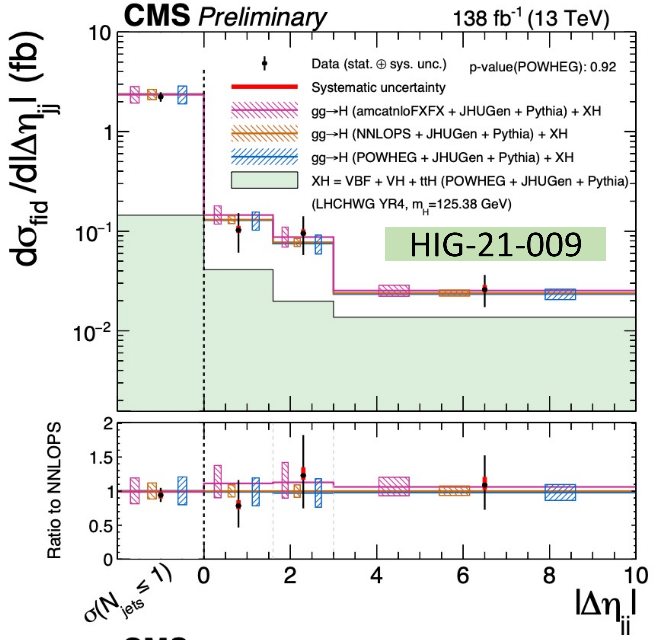

- Differential observables of **Jet activity**
  - Mass and distance of the di-jets
  - Mass and p_T of H + j systems
  - Mass of H + di-jets systems
  - To exploit the dedicated phase region

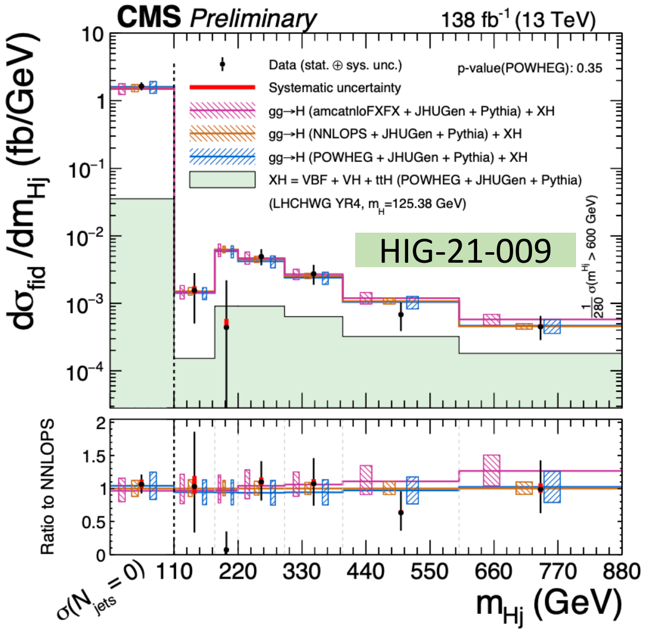

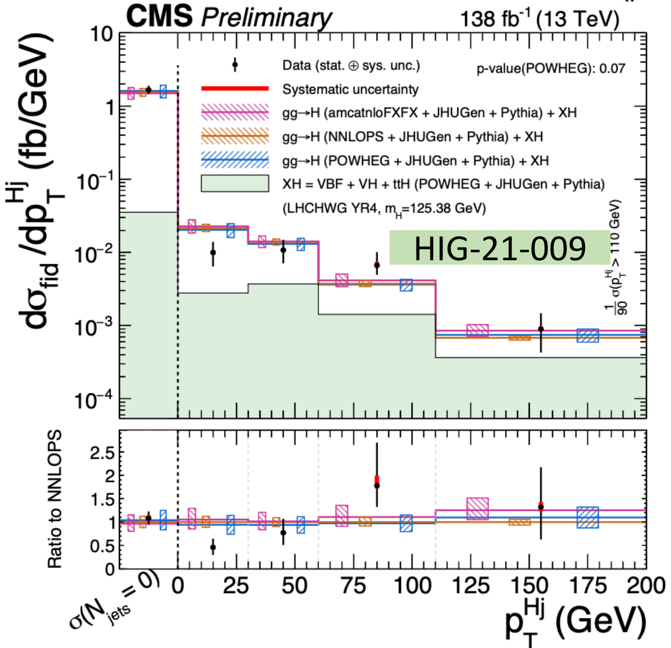

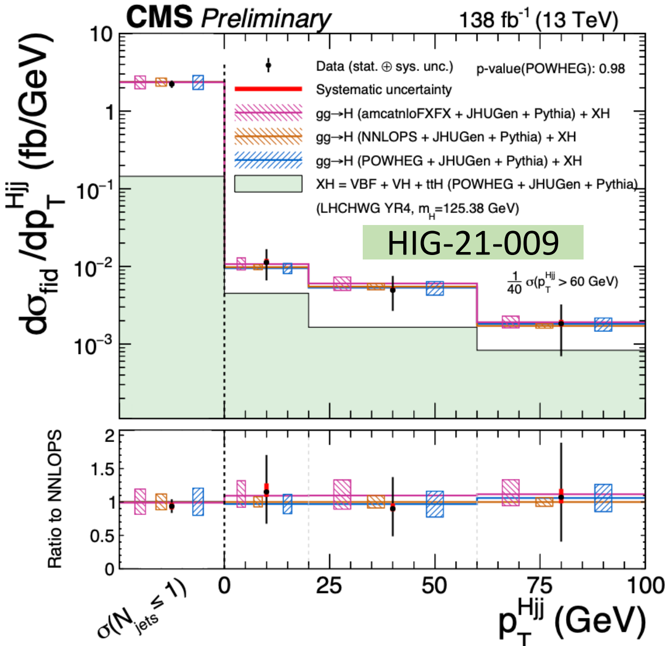

Results of measurements

Inclusive fiducial cross section

Irreducible background normalization taken from MC simulation and ZZ floating in the fit

Interpretations

k_{λ}, k_b, k_c

Differential observables Higgs Production

p_T^H $|y_H|$

N_{jets} p_T^{j1} p_T^{j2} m_{jj} $|\Delta\eta_{jj}|$

p_T^{Hj} m_{Hj} p_T^{Hjj} $\mathcal{T}_B$ $\mathcal{T}_C$

Differential observables Higgs decay

m_{Z1} m_{Z2}

Φ Φ_1 $\cos\theta$ $\cos\theta_1$ $\cos\theta^*$

$\mathcal{D}_{0-}^{\text{dec}}$ $\mathcal{D}_{cp}^{\text{dec}}$ $\mathcal{D}_{0h+}^{\text{dec}}$ $\mathcal{D}_{\Lambda1}^{\text{dec}}$ $\mathcal{D}_{\Lambda1}^{Z\gamma,\text{dec}}$ $\mathcal{D}_{int}^{\text{dec}}$

Double differential observables

m_{Z1} vs m_{Z2} N_{jets} vs p_T^H

$\mathcal{T}_C$ vs p_T^H $|y^H|$ vs p_T^H

p_T^{Hj} vs p_T^H p_T^{j1} vs p_T^{j2}

Results of 1D Differential Cross Section

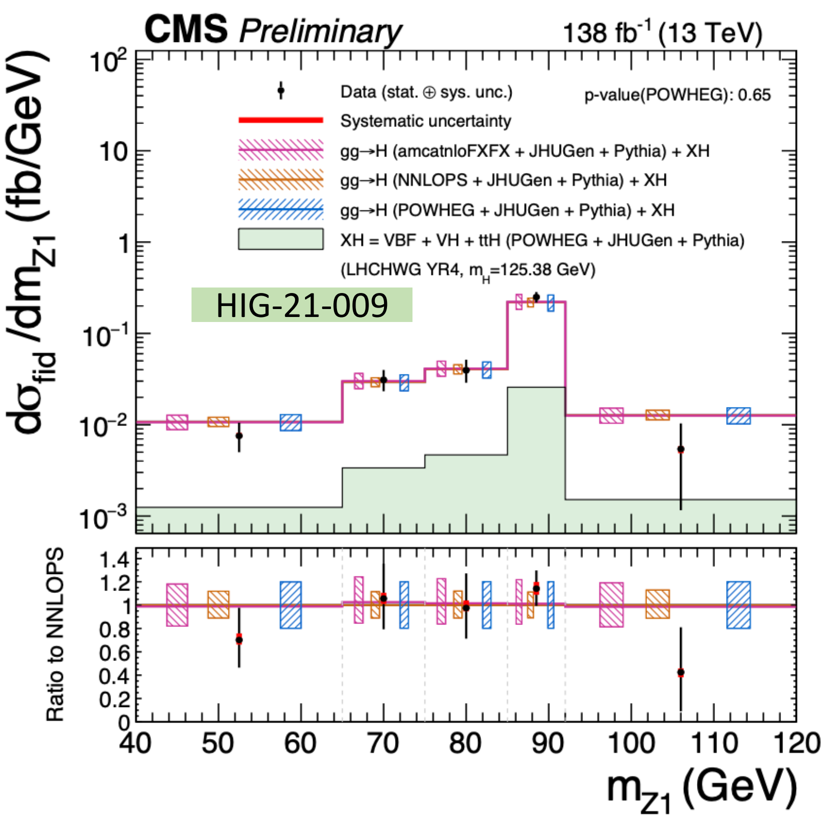

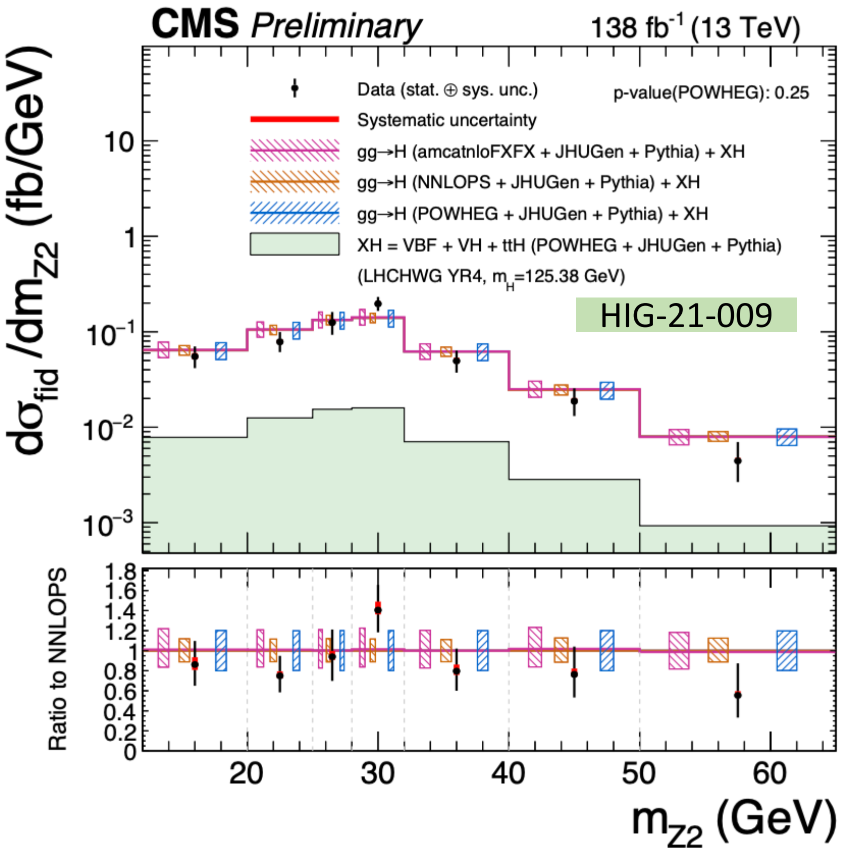

- Differential observables of **Higgs decay**
  - Mass of Z1
  - Mass of Z2
- Since the final state is sensitive to ***interference effects***, differential cross sections of decay are also measured in the **same-flavor** and **different flavor** final states.

Results of 1D Differential Cross Section

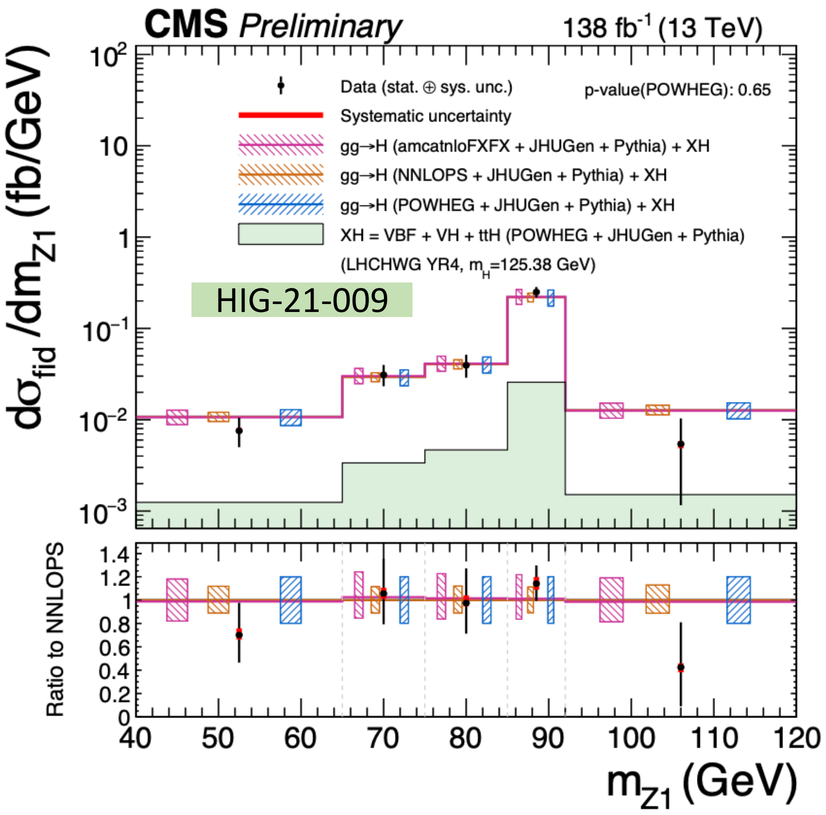

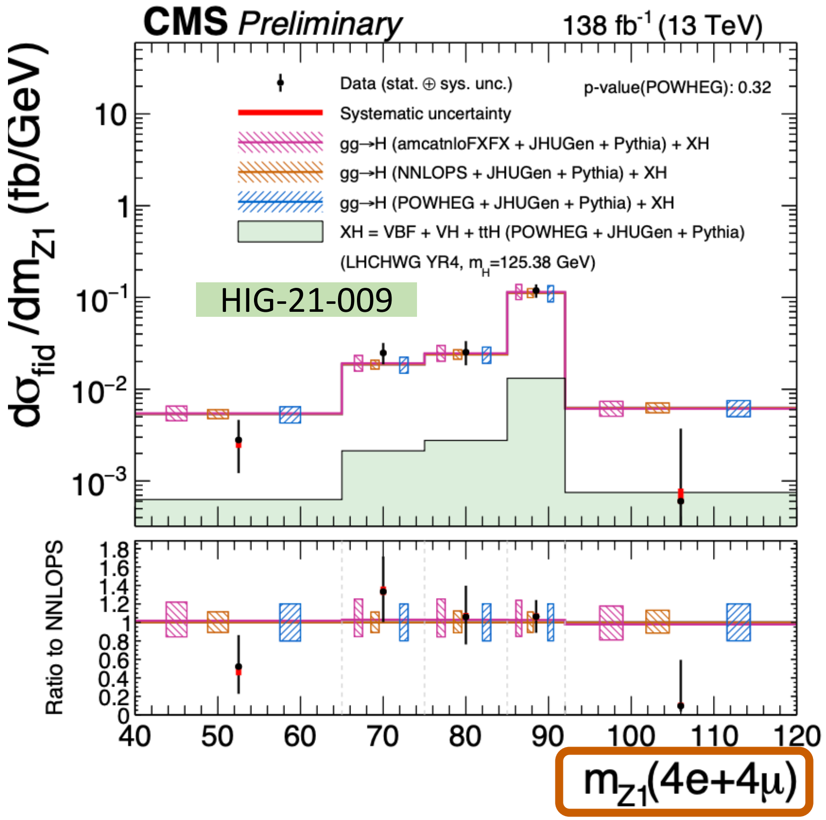

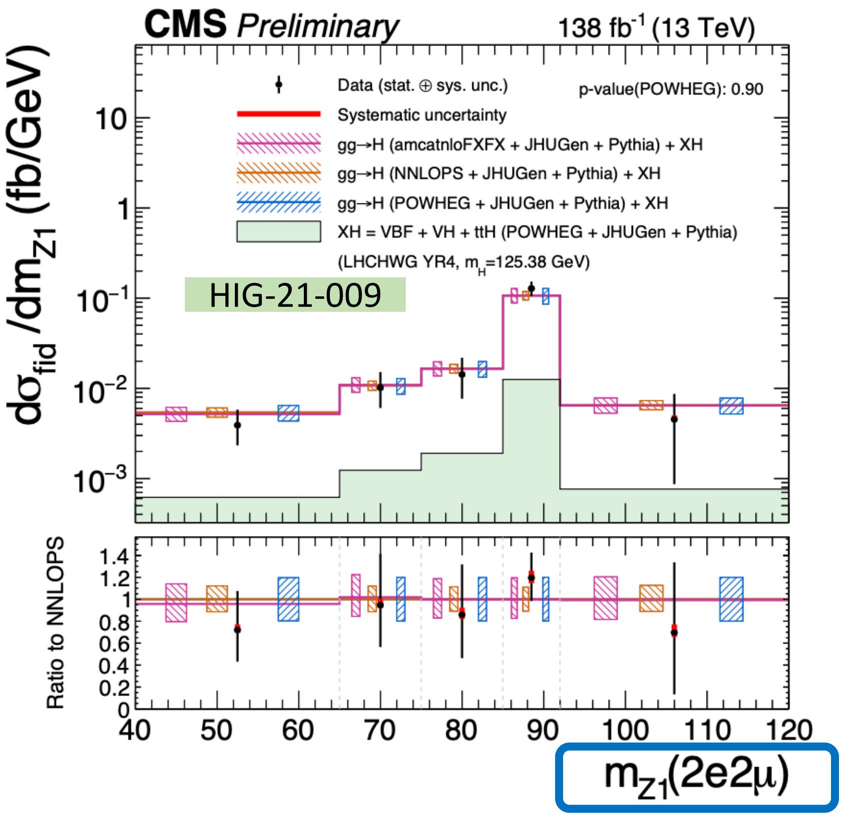

- Differential observables of **Higgs decay**
  - Mass of Z1
  - Mass of Z2
- Since the final state is sensitive to ***interference effects***, differential cross sections of decay are also measured in the **same-flavor** and **different flavor** final states.

1D differential cross section measurements

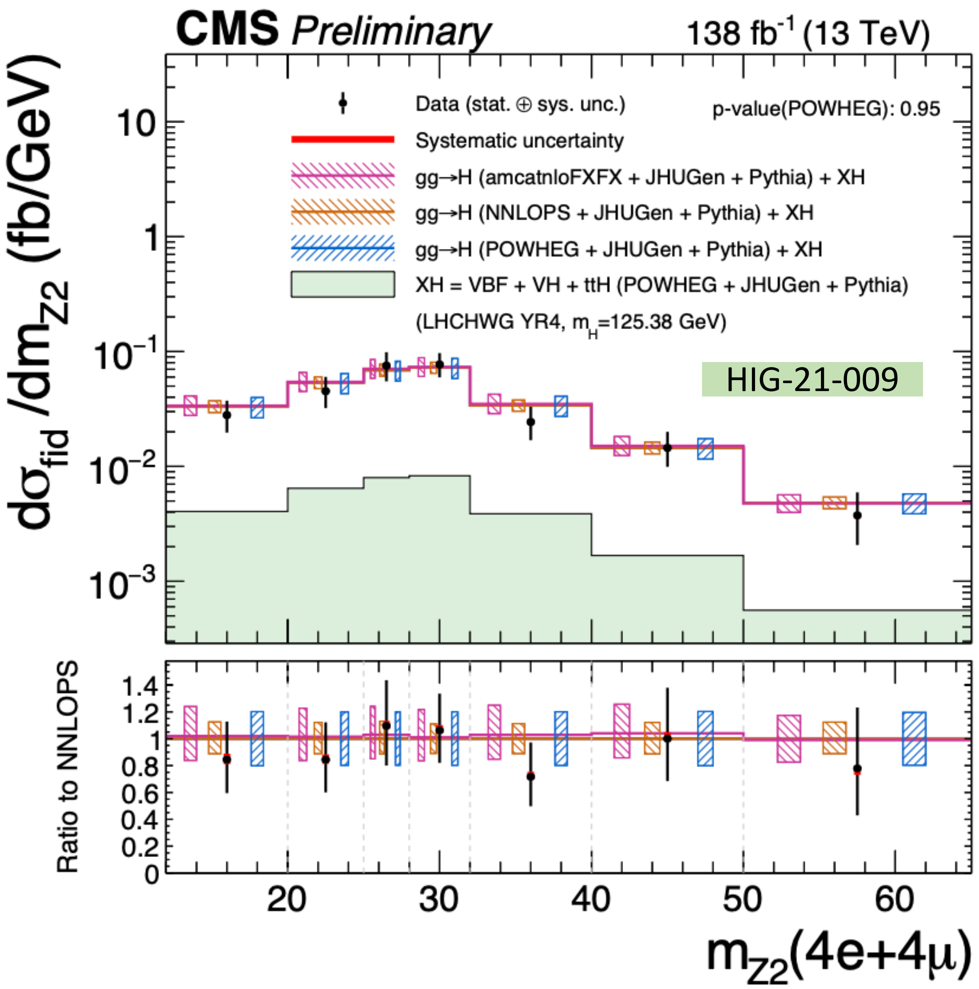

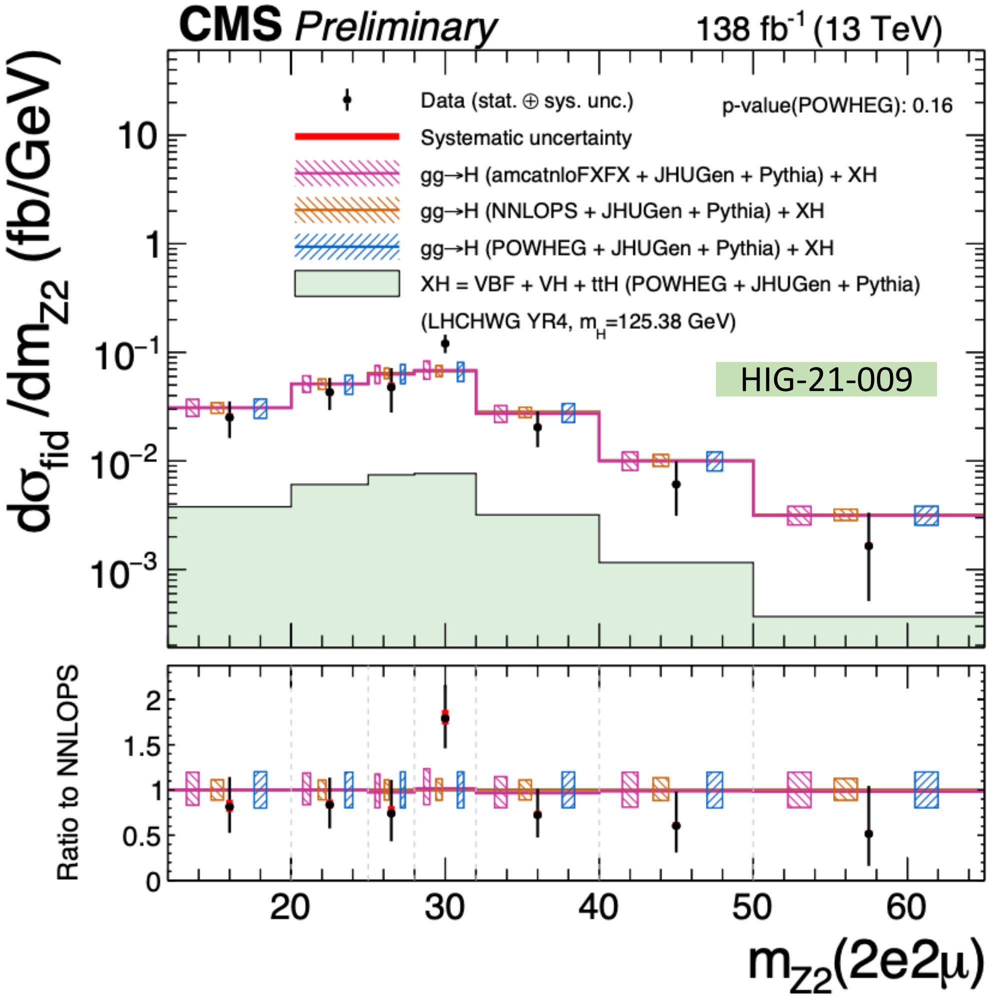

- Differential cross sections as a function of the invariant mass of the sub-leading di-lepton pair $m_{Z2}^{4e+4\mu}$ in the same-flavor (left) and different flavor $m_{Z2}^{2e2\mu}$ (right).

Decay observables

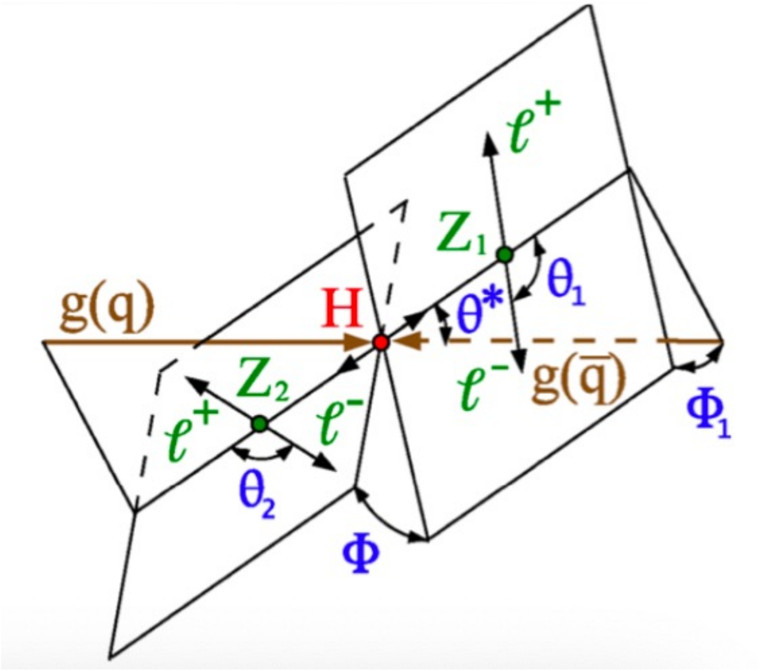

- Differential observables of **Higgs decay**
  - Angular observables: $\Phi \quad \Phi_1 \quad \cos\theta \quad \cos\theta_1 \quad \cos\theta^*$
  - Describe angle between the plane of Higgs, Z_1, Z_2 decay and the beam direction
  - Sensitive to the spin and charge conjugation and parity properties of the Higgs

1D Differential Cross Section --- Decay

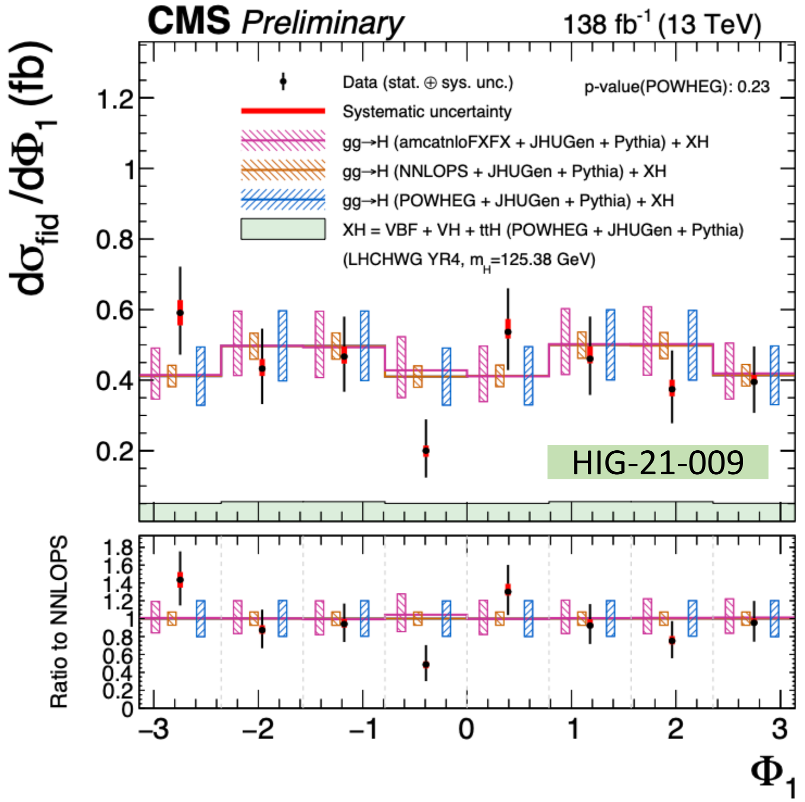

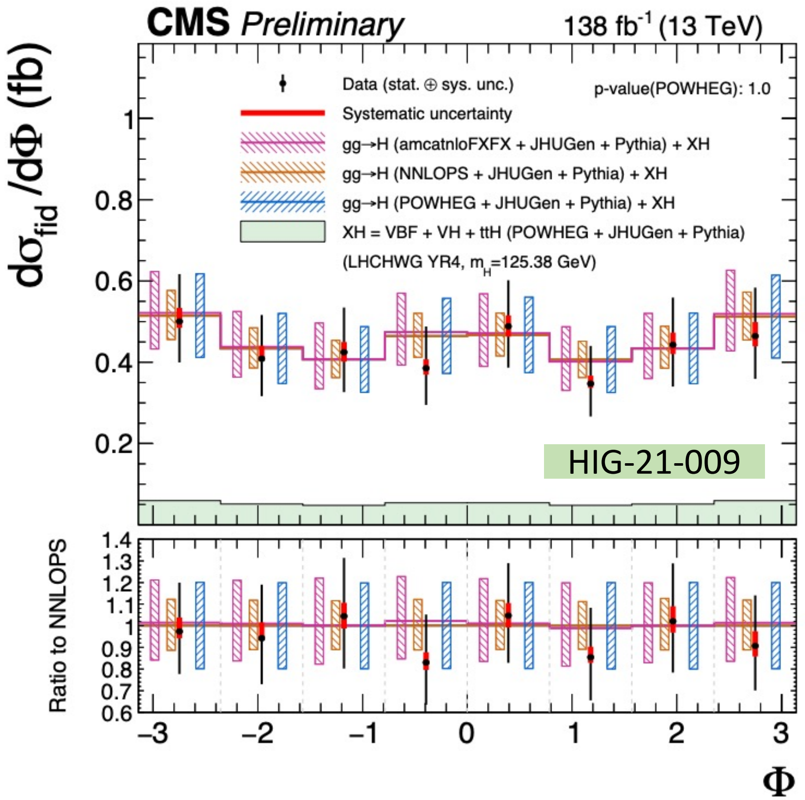

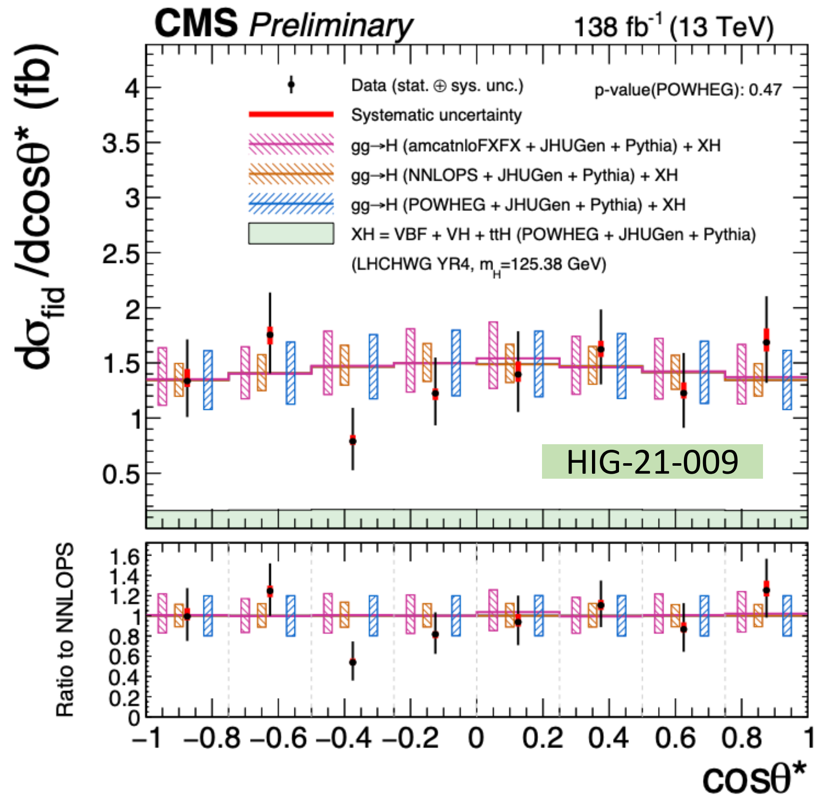

- Differential observables of **Higgs decay**
  - Φ_1 Φ $\cos\theta^*$
  - Sensitive to the spin and charge conjugation and parity properties of the Higgs

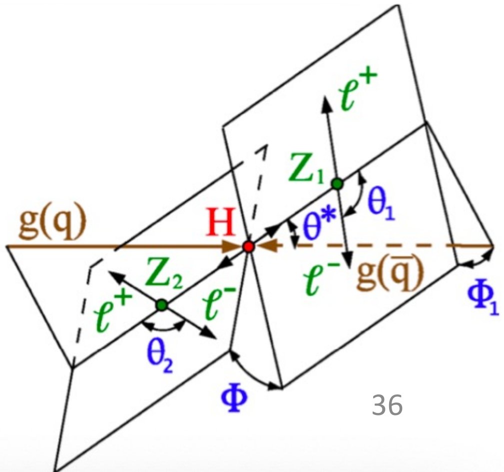

1D Differential Cross Section --- Decay

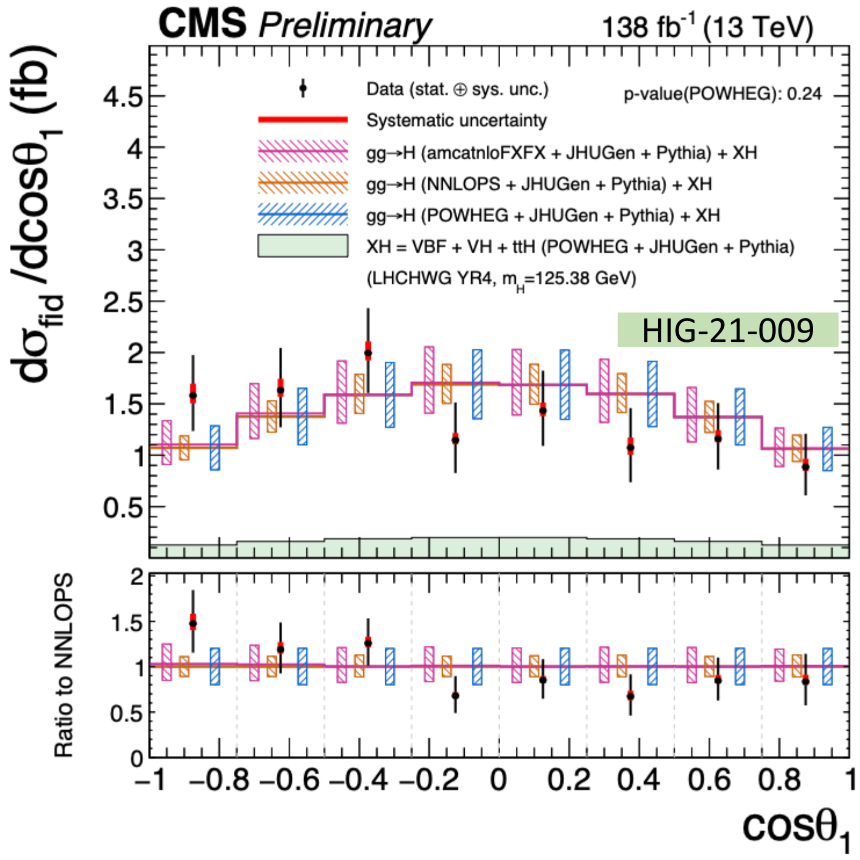

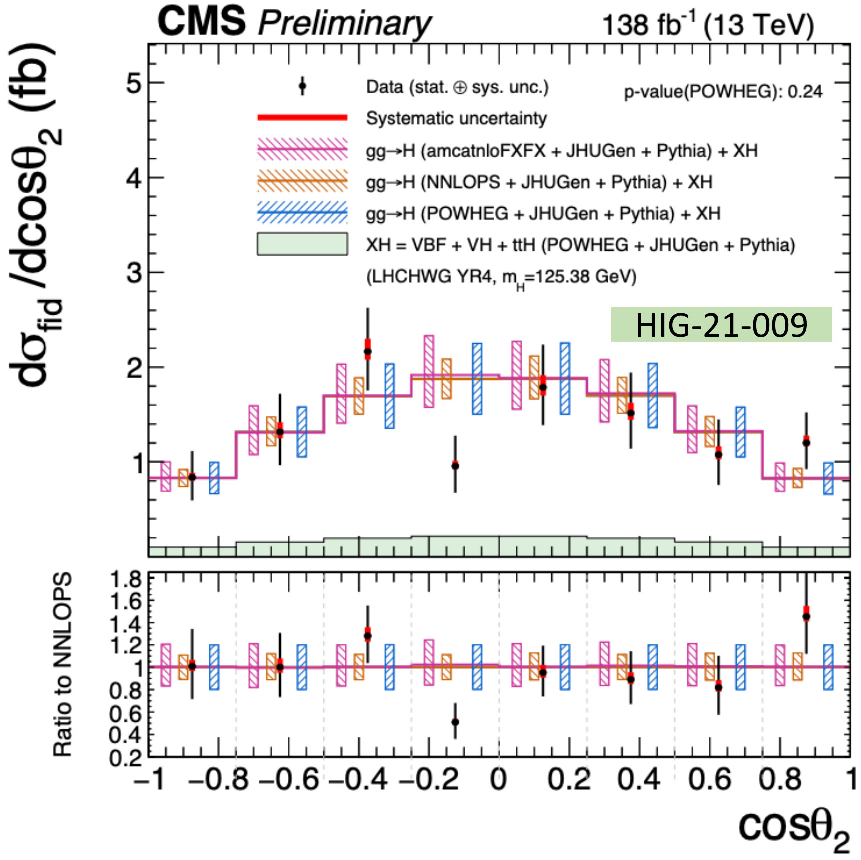

- Differential observables of **Higgs decay**
  - $\cos\theta_1, \cos\theta_2$
  - Sensitive to the spin and charge conjugation and parity properties of the Higgs

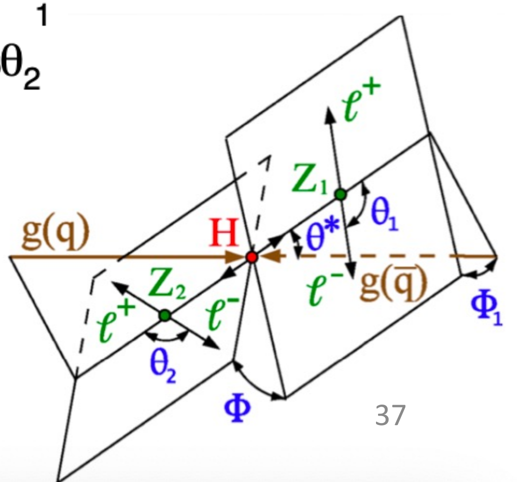

1D differential cross section measurements

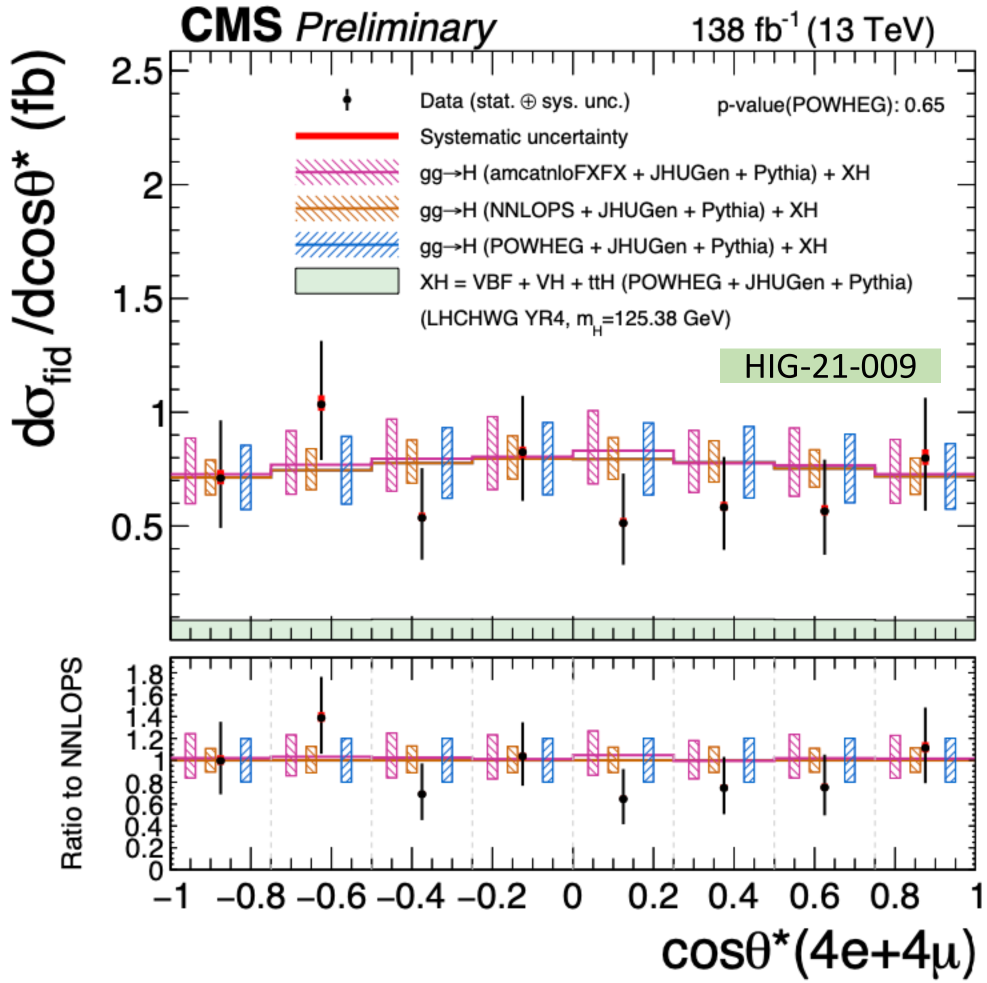

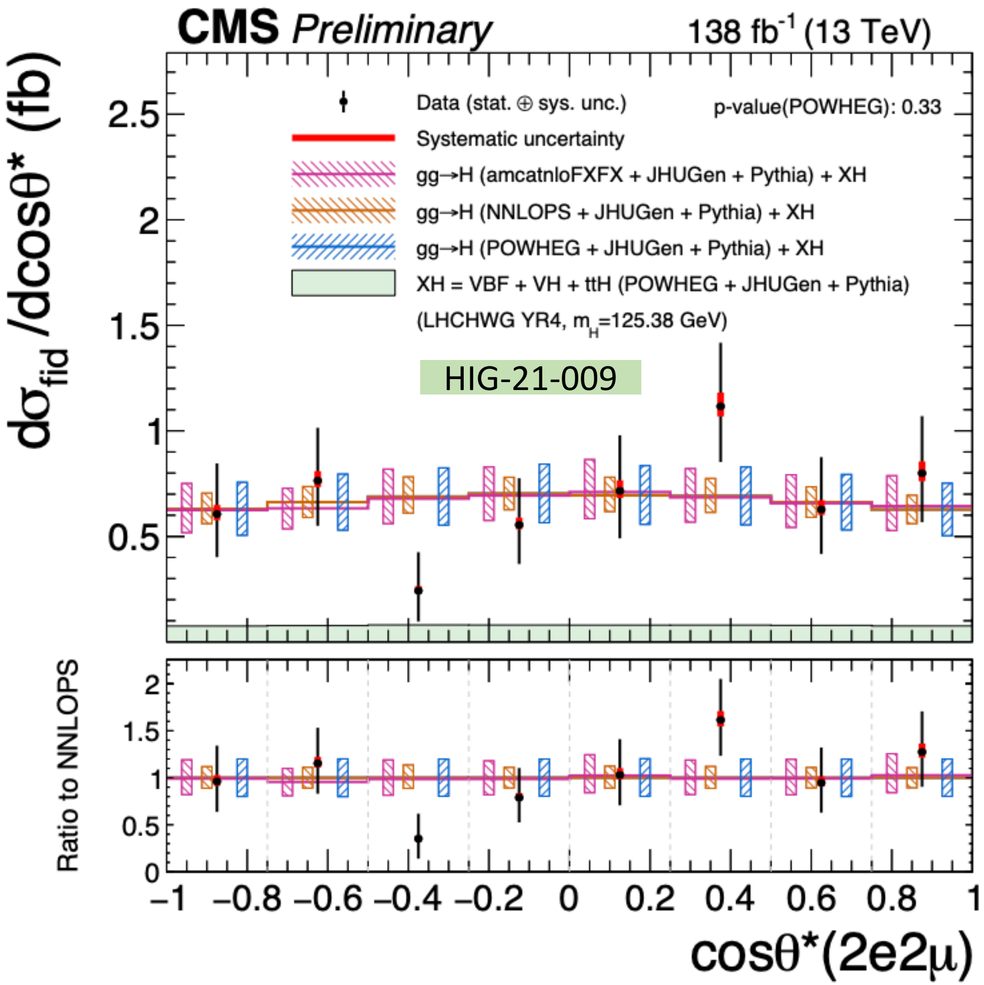

- Differential cross sections as a function of $cos\theta^*_{4e+4\mu}$ in the same-flavor (left) and different flavor $cos\theta^*_{2e2\mu}$(right).

1D differential cross section measurements

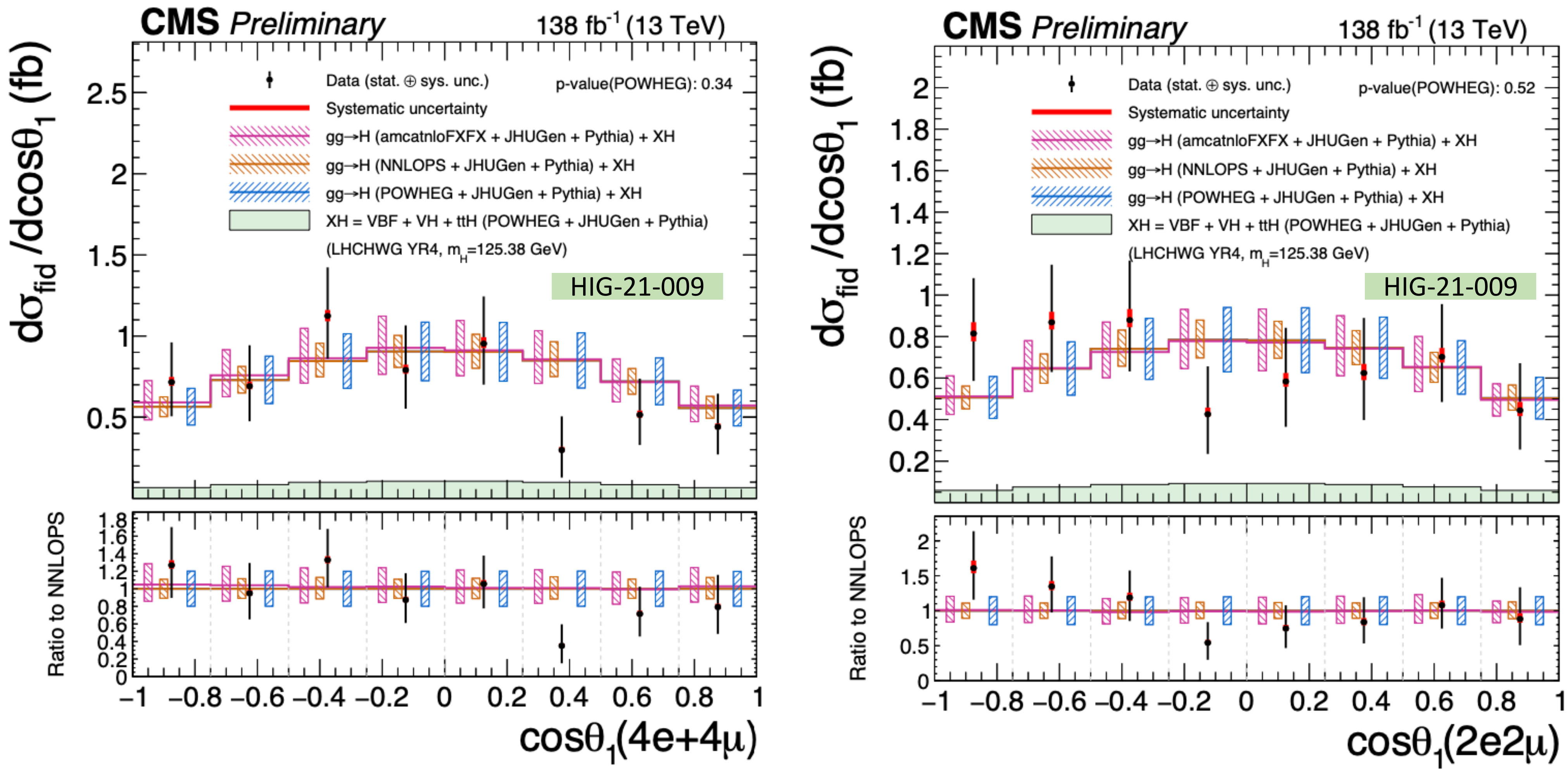

- Differential cross sections as a function of $cos\theta_1^{4e+4\mu}$ in the same-flavor (left) and different flavor $cos\theta_1^{2e2\mu}$(right).

1D differential cross section measurements

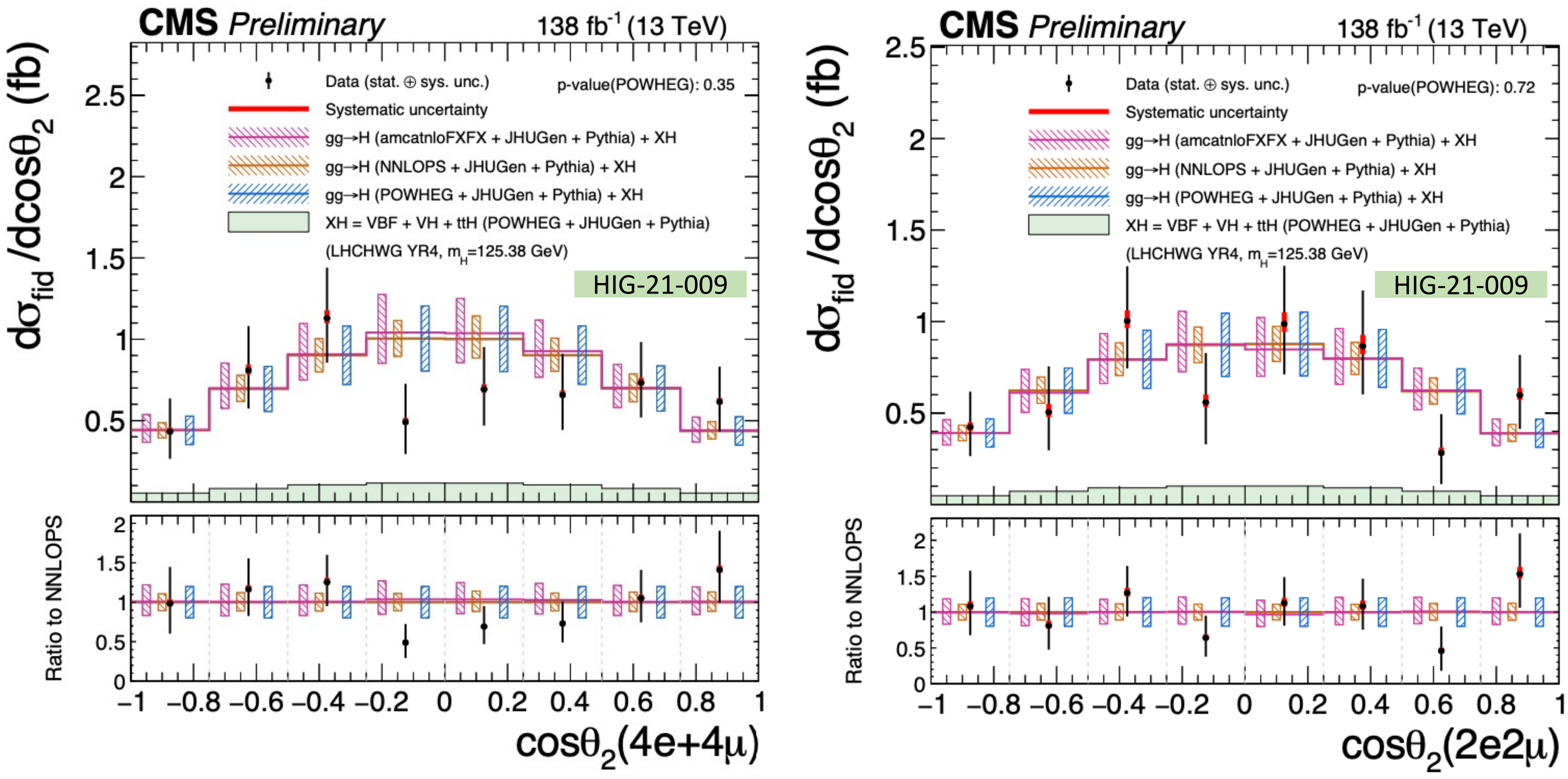

- Differential cross sections as a function of $cos\theta_2^{4e+4\mu}$ in the same-flavor (left) and different flavor $cos\theta_2^{2e2\mu}$(right).

1D differential cross section measurements

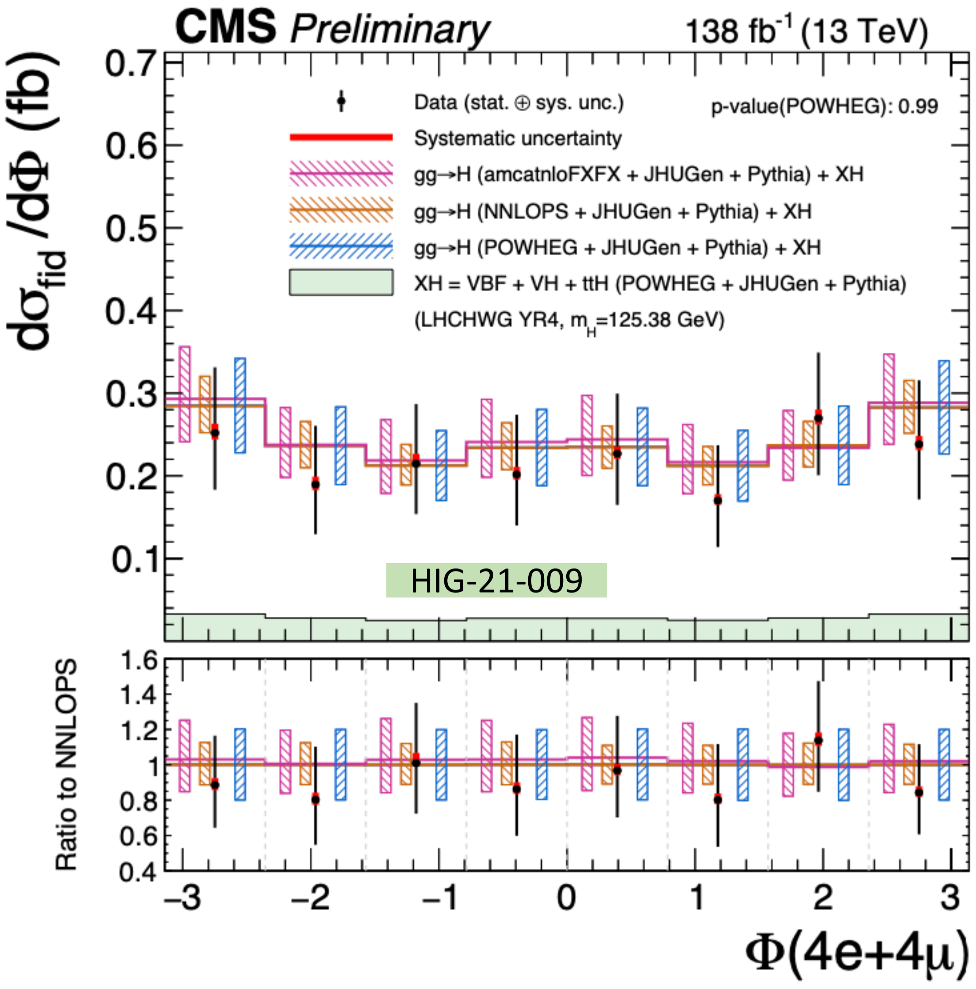

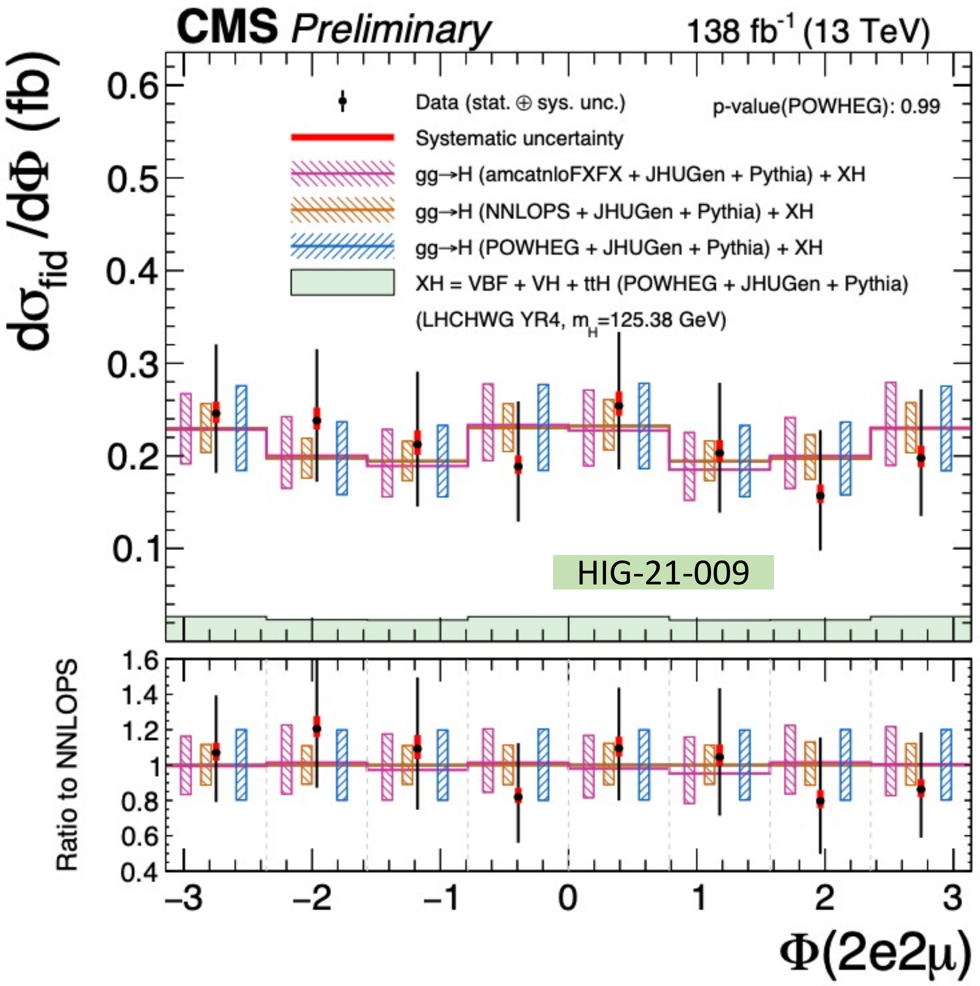

- Differential cross sections as a function of angle $\Phi_{4e+4\mu}$ in the same-flavor (left) and different flavor $\Phi_{2e2\mu}$ (right).

1D differential cross section measurements

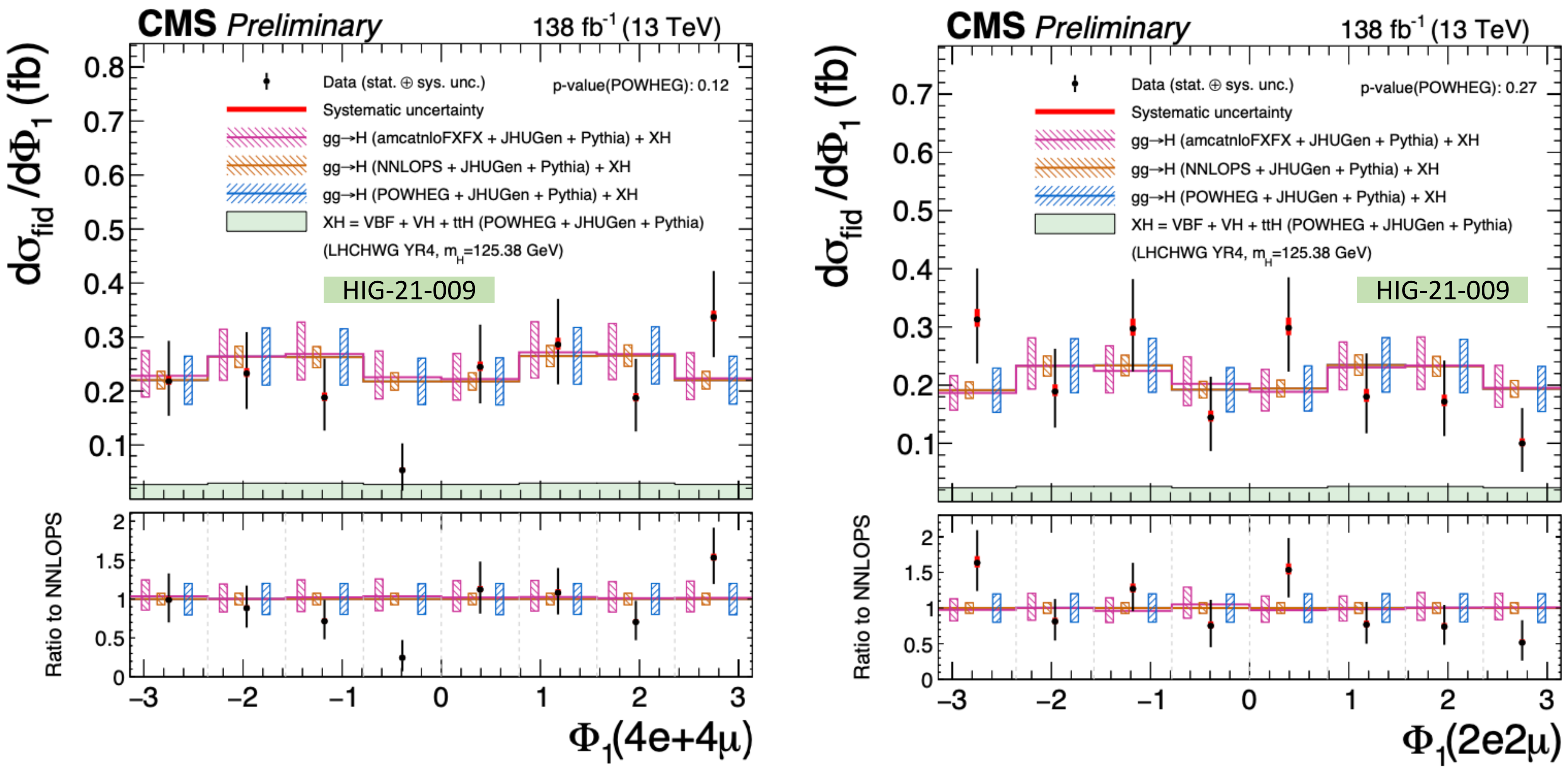

- Differential cross sections as a function of angle $\Phi_1^{4e+4\mu}$ in the same-flavor (left) and different flavor $\Phi_1^{2e2\mu}$ (right).

1D Differential Cross Section --- Decay

- Higgs **Decay** in 4l final states could be characterized by the following seven parameters:
  - m_{Z1}, m_{Z2}
  - Φ , Φ_1 , $\cos\theta$, $\cos\theta_1$, $\cos\theta^*$

☆ $\mathcal{D}_{0-}^{\rm dec}$ $\mathcal{D}_{0h+}^{\rm dec}$ $\mathcal{D}_{\Lambda 1}^{\rm dec}$ $\mathcal{D}_{\Lambda 1}^{Z\gamma,\rm dec}$ | $\mathcal{D}_{cp}^{\rm dec}$ $\mathcal{D}_{int}^{\rm dec}$

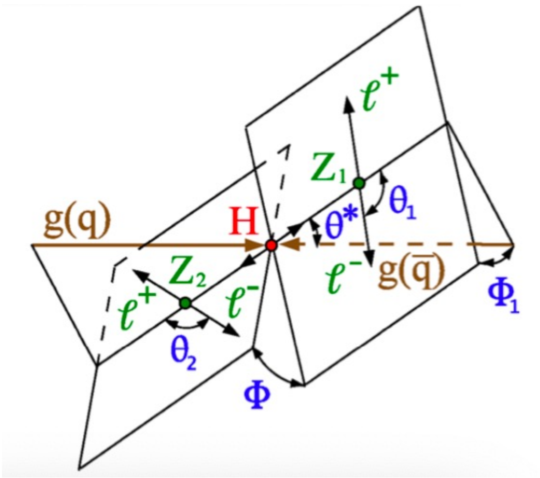

1D Differential Cross Section --- Decay

- Higgs **Decay** in 4l final states could be characterized by the following seven parameters:
  - m_{Z1}, m_{Z2}
  - $\Phi\,,\ \Phi_1\,,\ \cos\theta\,,\ \cos\theta_1\,,\ \cos\theta^*$

☆ $\mathcal{D}_{0-}^{\text{dec}}$ $\mathcal{D}_{0h+}^{\text{dec}}$ $\mathcal{D}_{\Lambda1}^{\text{dec}}$ $\mathcal{D}_{\Lambda1}^{Z\gamma,\text{dec}}$ | $\mathcal{D}_{cp}^{\text{dec}}$ $\mathcal{D}_{int}^{\text{dec}}$

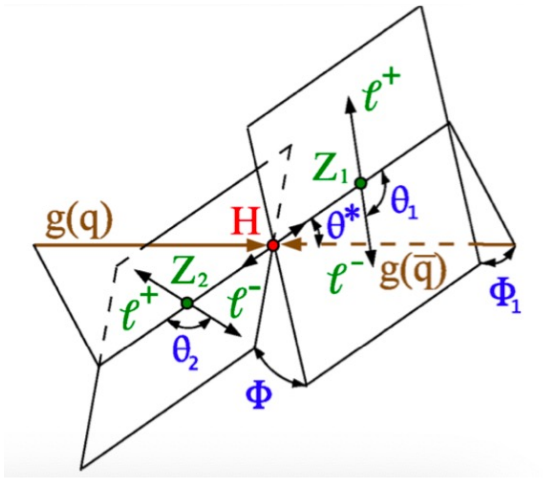

- HVV scattering amplitude of a spin-0 boson H and two spin-one gauge bosons

$$A(HV_1V_2) = \frac{1}{v}\left[a_1^{VV} + \frac{k_1^{VV} q_{V1}^2 + k_2^{VV} q_{V2}^2}{(\Lambda_1^{VV})^2} + \frac{k_3^{VV}(q_{V1}+q_{V2})^2}{(\Lambda_Q^{VV})^2}\right] m_{V1}^2 \epsilon_{V1}^* \epsilon_{V2}^* + a_2^{VV} f_{\mu\nu}^{*(1)} f^{*(2),\mu\nu} + a_3^{VV} f_{\mu\nu}^{*(1)} \tilde{f}^{*(2),\mu\nu}$$

CP even
- SM-like spin-zero 0^+: $a_1^{ZZ}=a_1^{WW}=2$
- Higher order spin-zero 0_h^+: a_2

CP odd
- Pseudoscalar spin-zero 0^- : a_3

Scales of BSM physics

- Observables sensitive to HVV anomalous couplings using kinematics of leptons in decay

$$\mathcal{D}_{\text{alt}} = \frac{\mathcal{P}_{\text{sig}}(\vec{\Omega})}{\mathcal{P}_{\text{sig}}(\vec{\Omega}) + \mathcal{P}_{\text{alt}}(\vec{\Omega})} \qquad \mathcal{D}_{\text{int}} = \frac{\mathcal{P}_{\text{int}}(\vec{\Omega})}{2\cdot\sqrt{\mathcal{P}_{\text{sig}}(\vec{\Omega})\cdot\mathcal{P}_{\text{alt}}(\vec{\Omega})}},$$

	$\mathcal{D}_{\text{alt}}$				$\mathcal{D}_{\text{int}}$	
Coupling	a_3	a_2	κ_1	$\kappa_2^{Z,\gamma}$	a_3	a_2
Discriminant	$\mathcal{D}_{0-}$	$\mathcal{D}_{0h+}$	$\mathcal{D}_{\Lambda1}$	$\mathcal{D}_{\Lambda1}^{Z,\gamma}$	$\mathcal{D}_{\text{CP}}$	$\mathcal{D}_{\text{int}}$

1D Differential Cross Section --- Decay

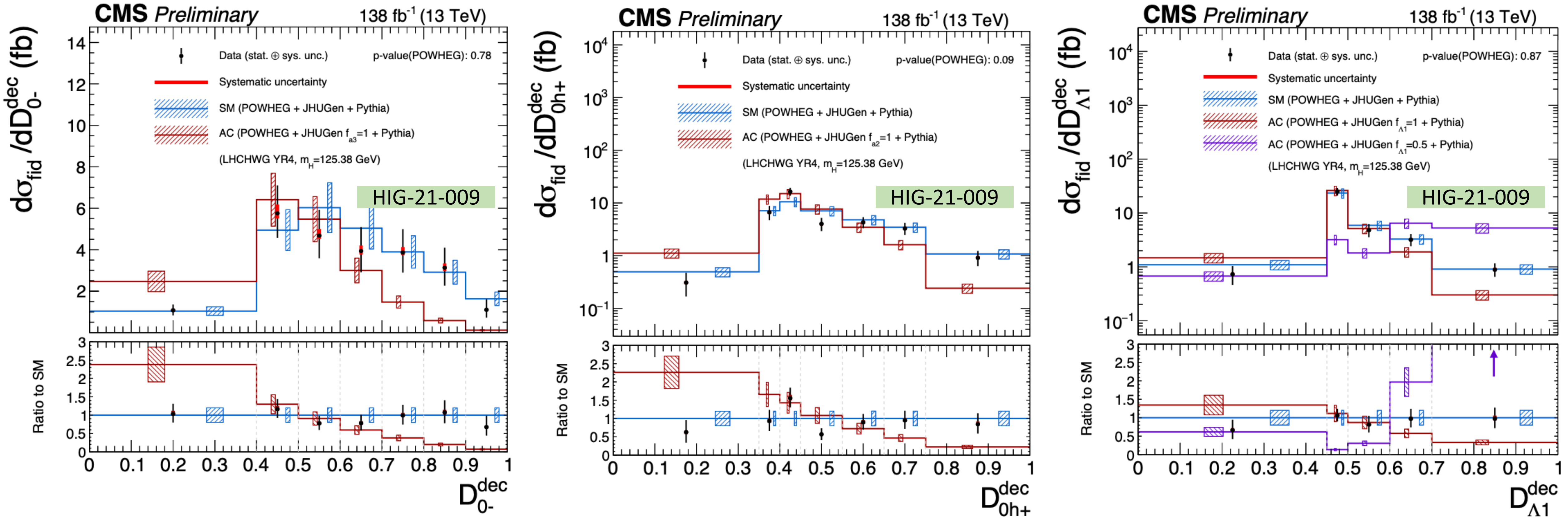

- Differential cross sections as a function of
  - Matrix-element discriminants
    - Built based on the two hypotheses for which the discriminant is designed for
      - Standard Model prediction ggH (POWHEG) + XH
      - Anomalous Coupling prediction ggH AC samples normalized to the ggH+XH SM cross section
  - Probe **HZZ vertex** and sensitive to BSM physics

1D Differential Cross Section --- Decay

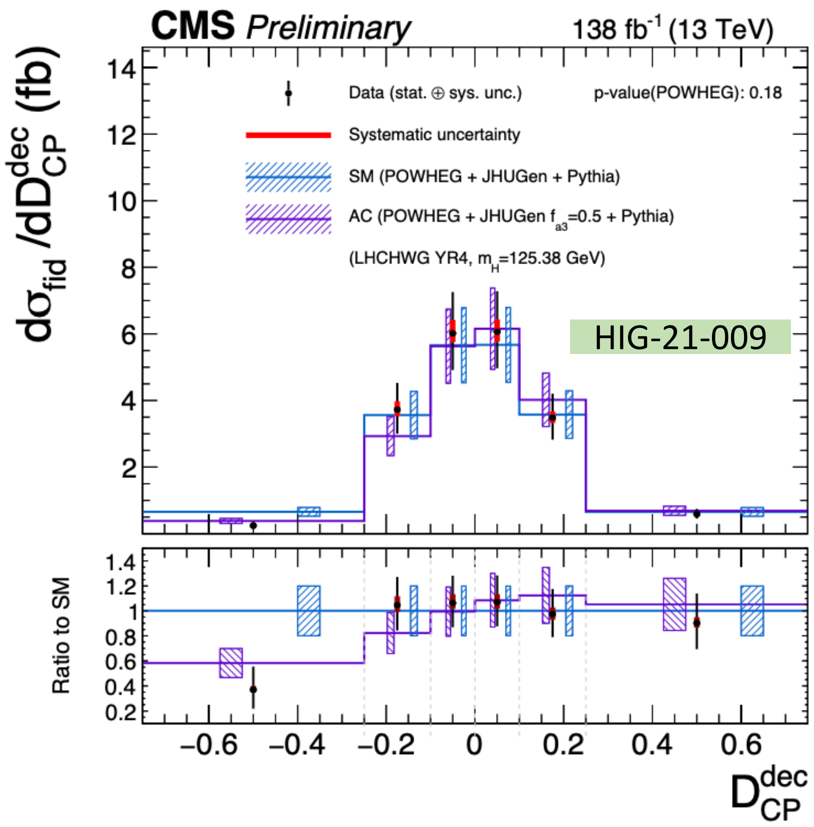

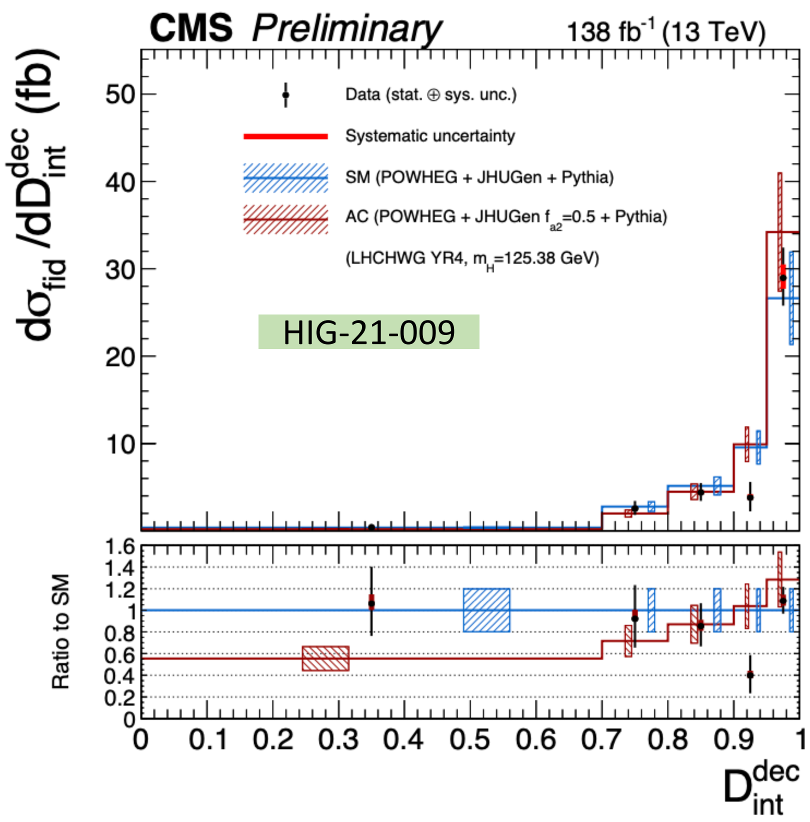

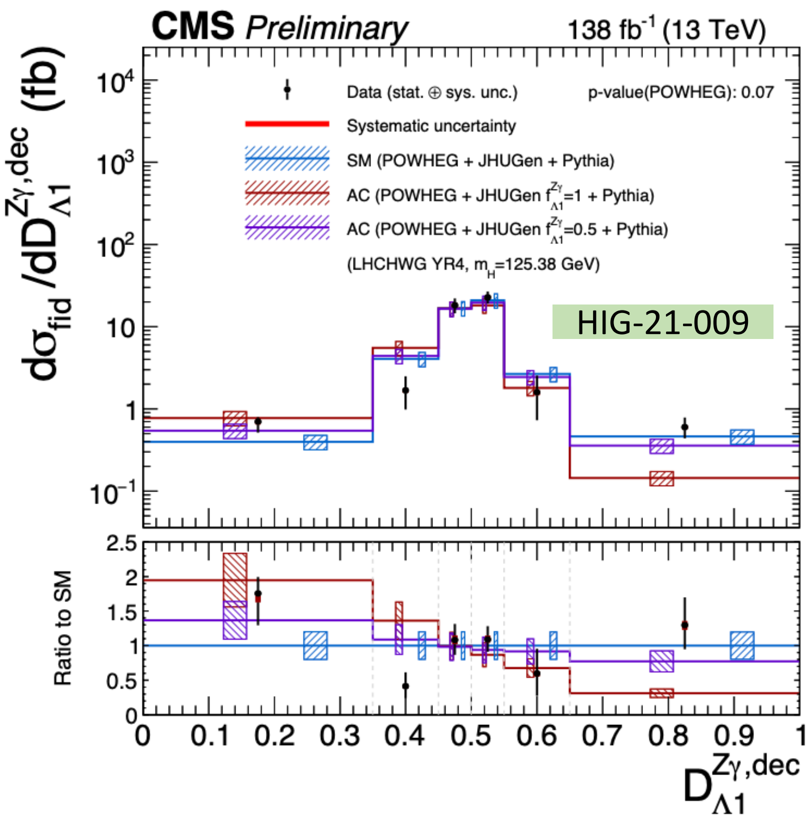

- Differential cross sections as a function of
  - Matrix-element discriminants
    - Built based on the two hypotheses for which the discriminant is designed for
      - Standard Model prediction ggH (POWHEG) + XH
      - Anomalous Coupling prediction ggH AC samples normalized to the ggH+XH SM cross section
  - Probe **HZZ vertex** and sensitive to BSM physics

1D differential cross section measurements

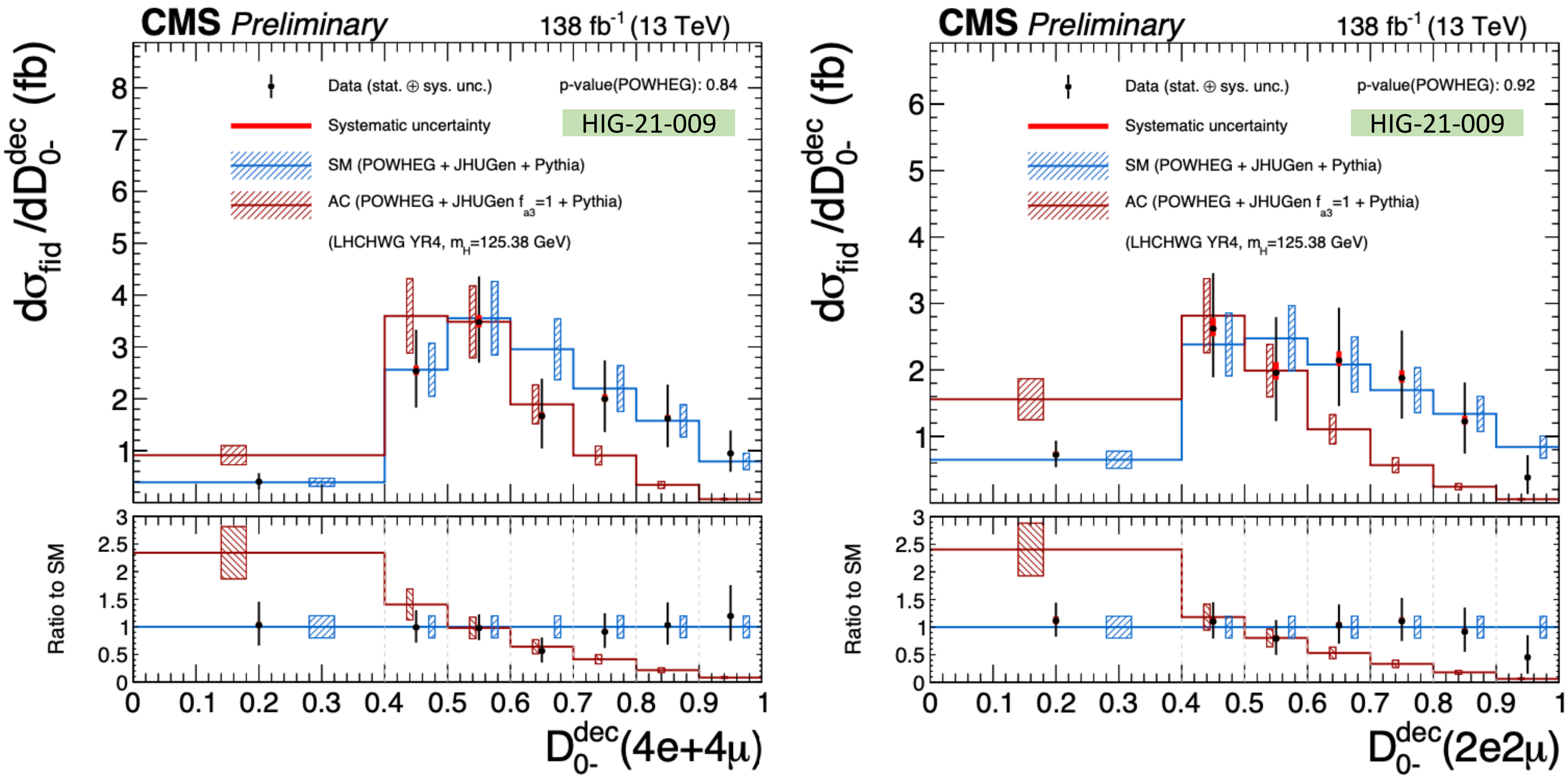

- Differential cross sections as a function of the matrix element kinematic discriminant $\mathcal{D}_{0-}^{dec}(4e+4\mu)$ in the same-flavor (left) and different flavor $\mathcal{D}_{0-}^{dec}(2e2\mu)$(right).

1D differential cross section measurements

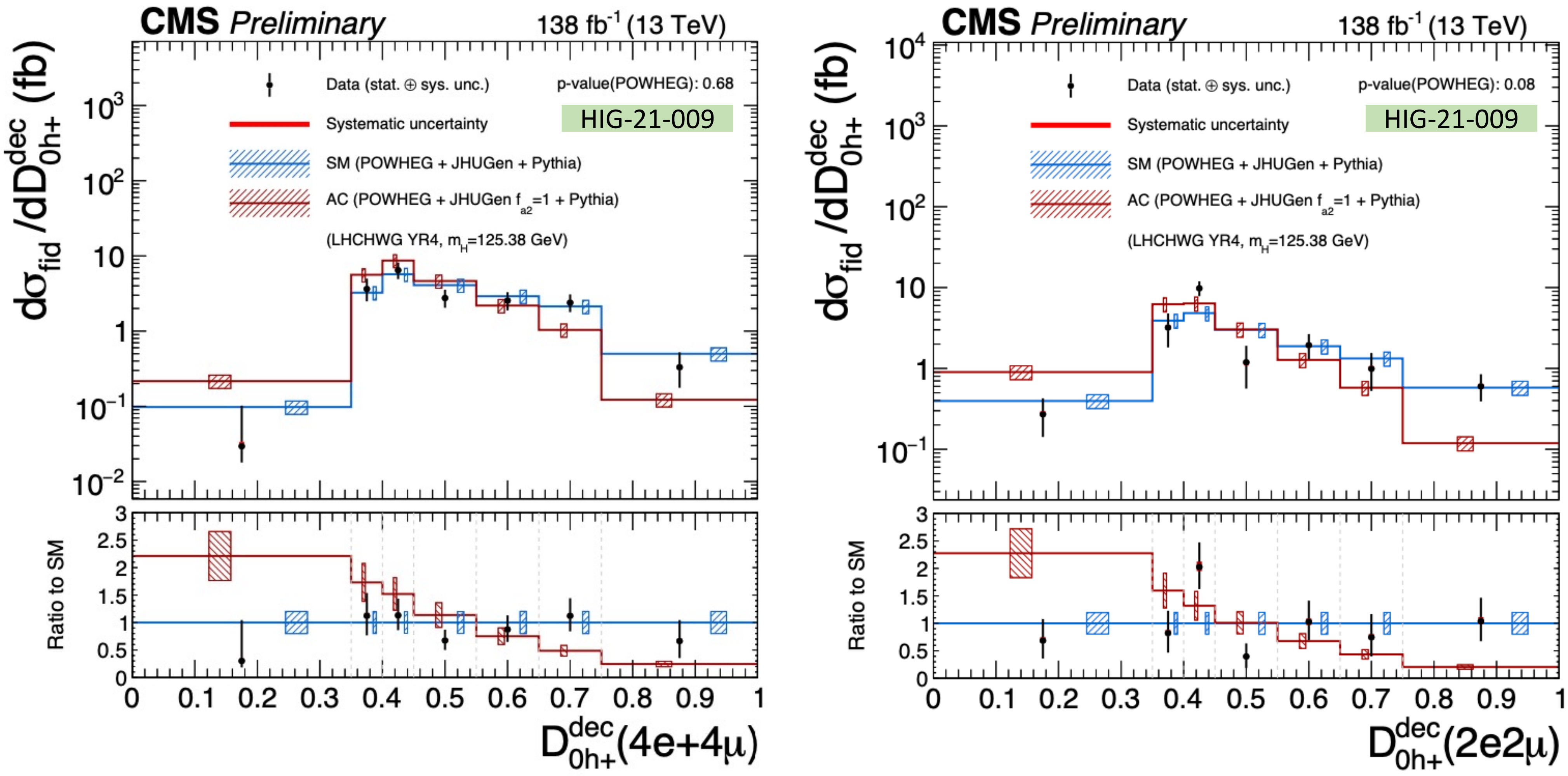

- Differential cross sections as a function of the matrix element kinematic discriminant $\mathcal{D}^{dec}_{0h+}(4e+4\mu)$ in the same-flavor (left) and different flavor $\mathcal{D}^{dec}_{0h+}(2e2\mu)$(right).

1D differential cross section measurements

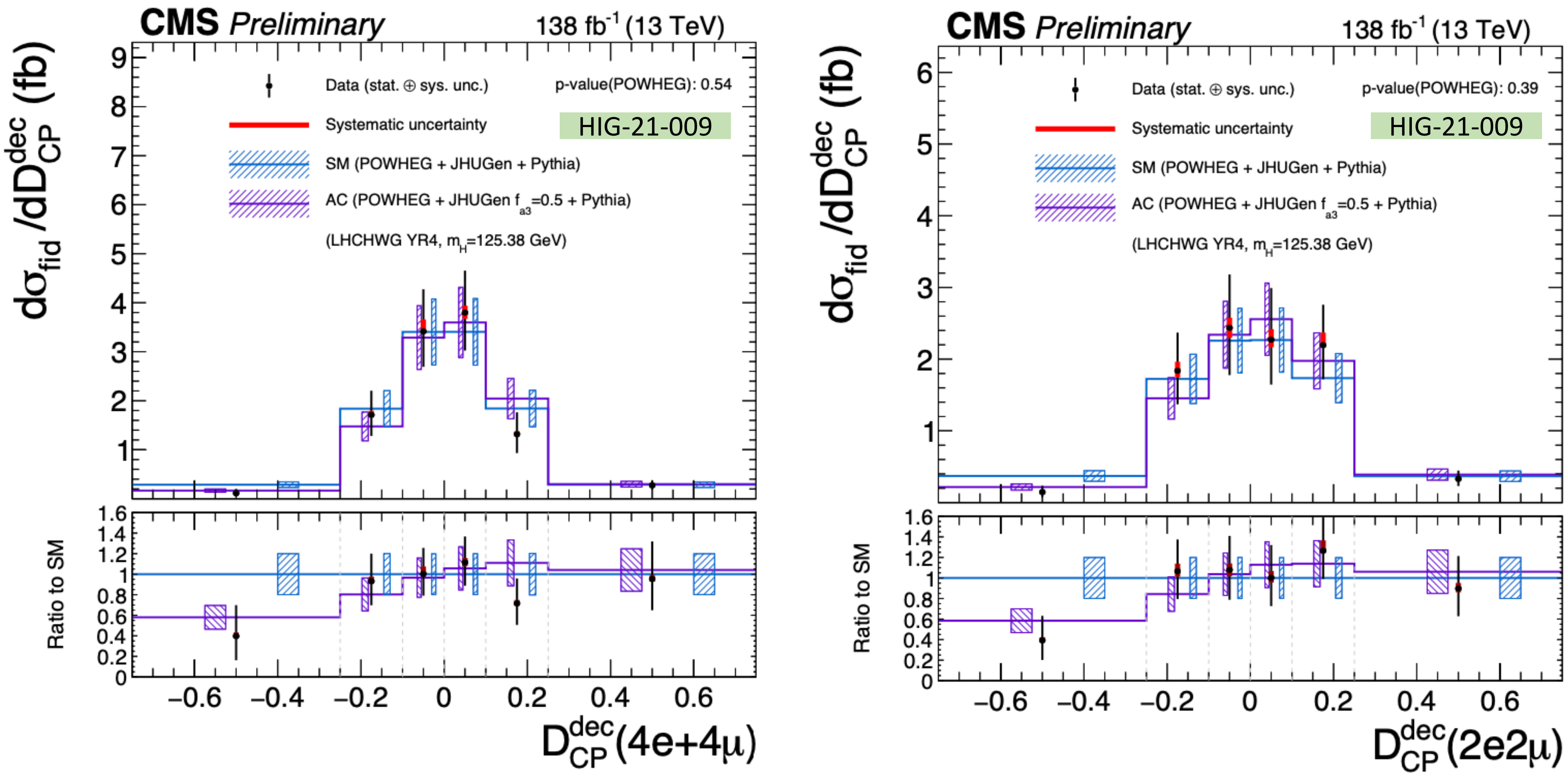

- Differential cross sections as a function of the matrix element kinematic discriminant $\mathcal{D}_{CP}^{dec}(4e+4\mu)$ in the same-flavor (left) and different flavor $\mathcal{D}_{CP}^{dec}(2e2\mu)$(right).

1D differential cross section measurements

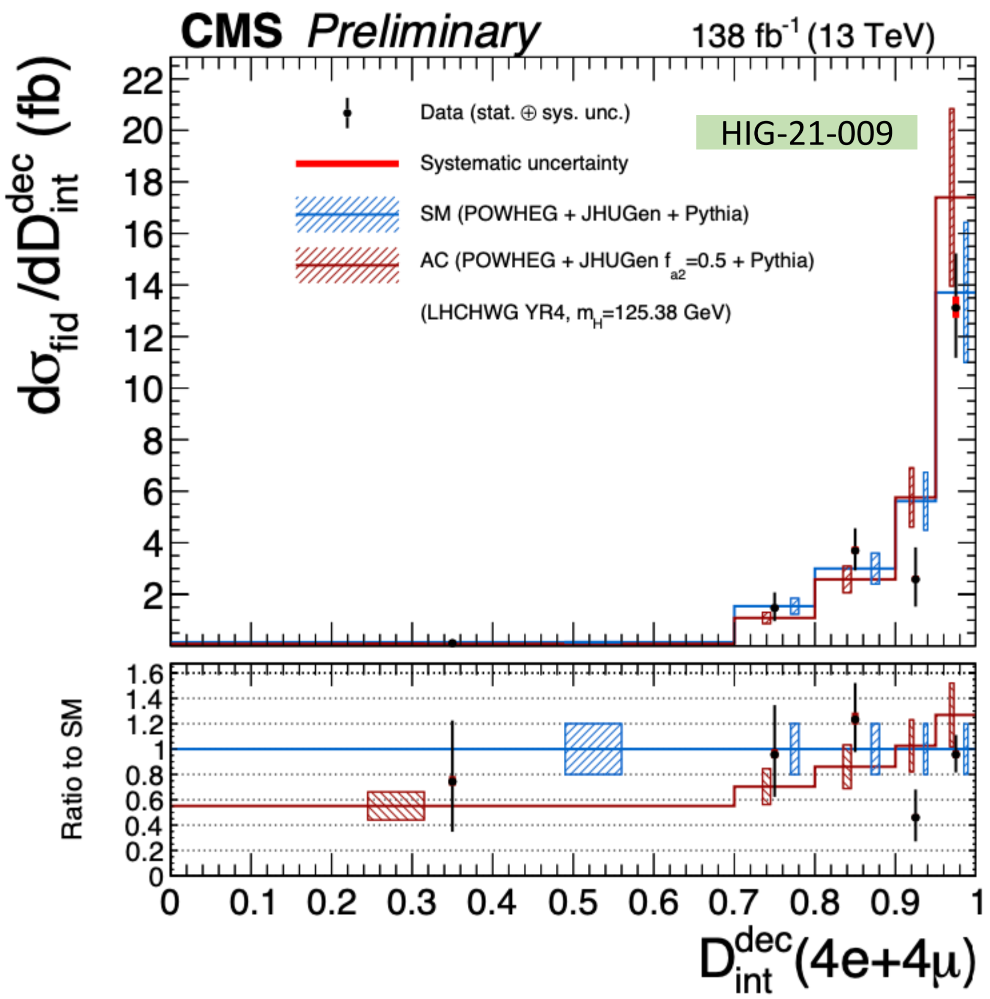

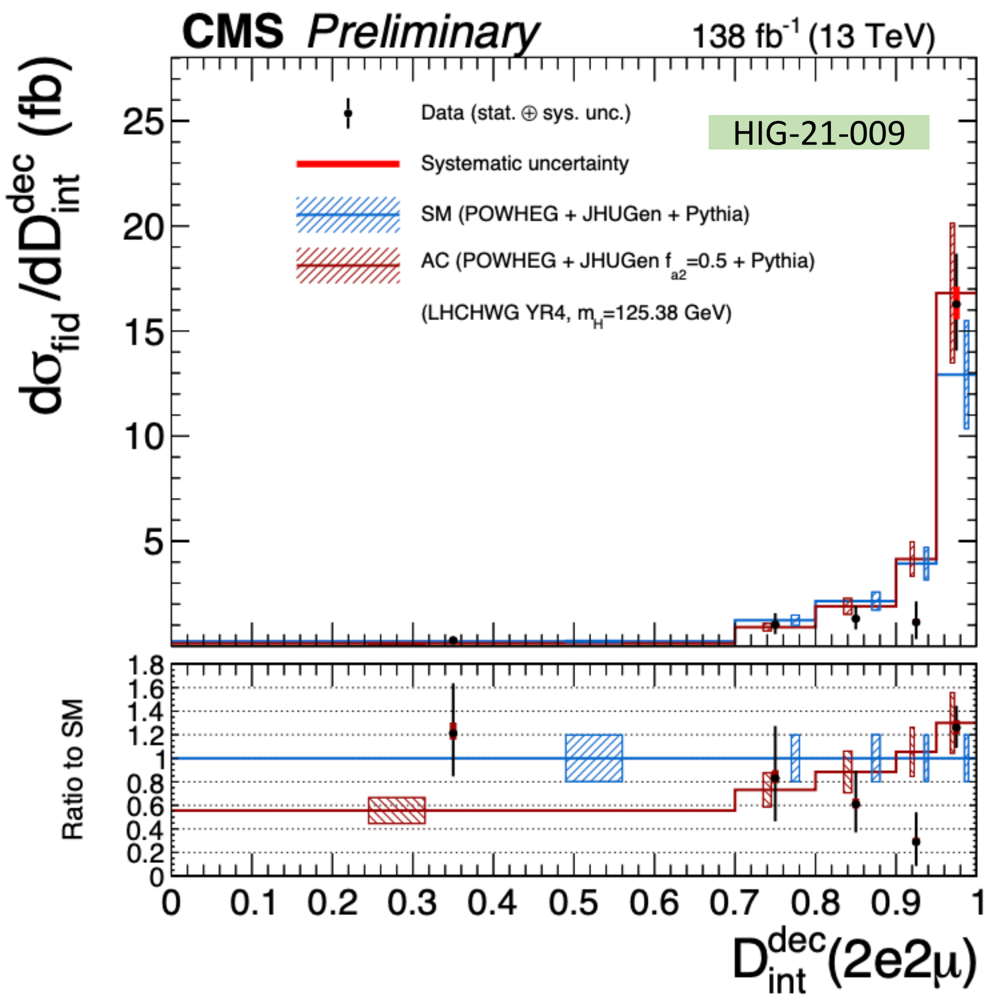

- Differential cross sections as a function of the matrix element kinematic discriminant $\mathcal{D}_{int}^{dec}(4e+4\mu)$ in the same-flavor (left) and different flavor $\mathcal{D}_{int}^{dec}(2e2\mu)$(right).

1D differential cross section measurements

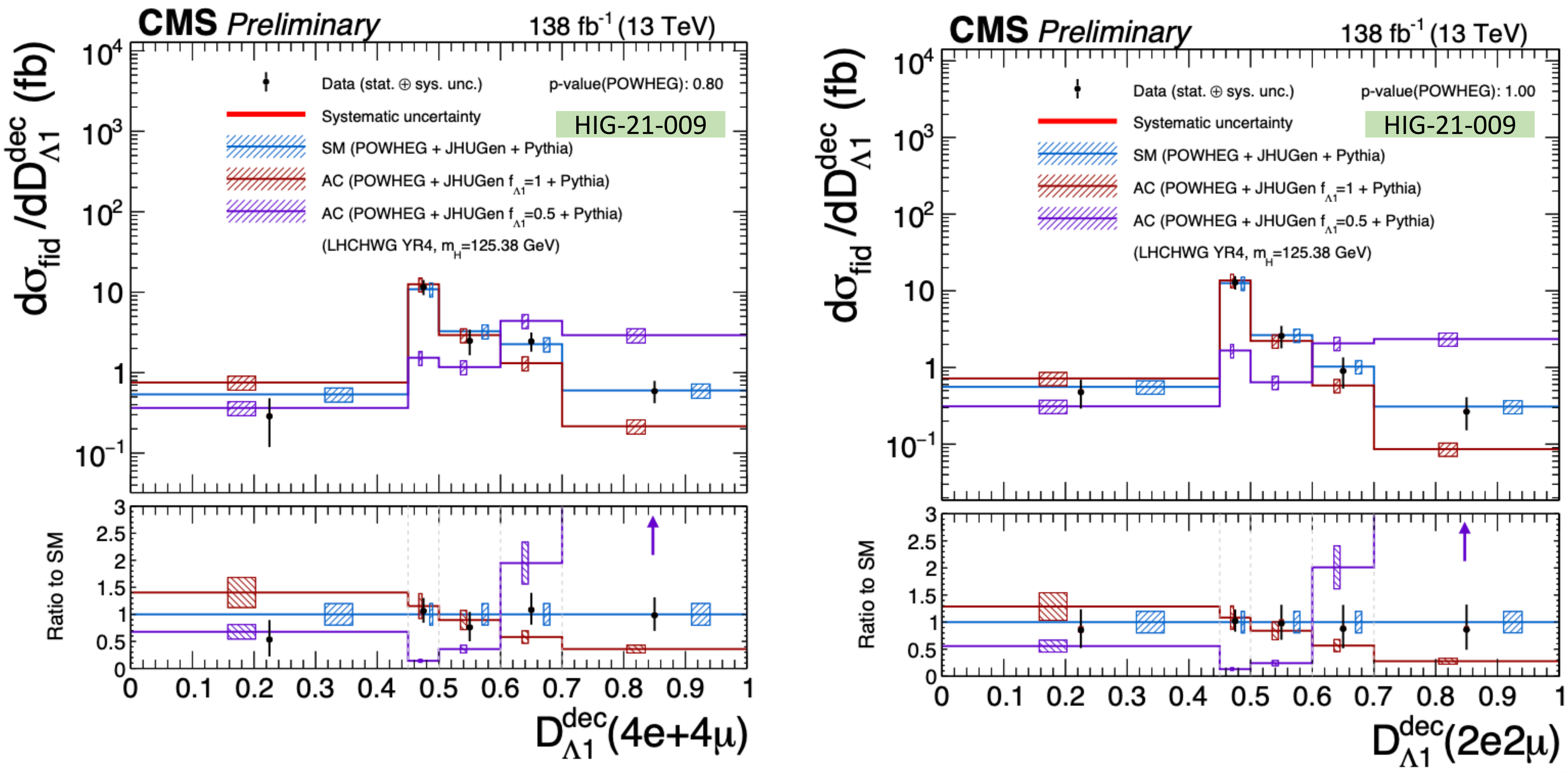

- Differential cross sections as a function of the matrix element kinematic discriminant $\mathcal{D}_{\Lambda 1}^{dec}(4e+4\mu)$ in the same-flavor (left) and different flavor $\mathcal{D}_{\Lambda 1}^{dec}(2e2\mu)$(right).

1D differential cross section measurements

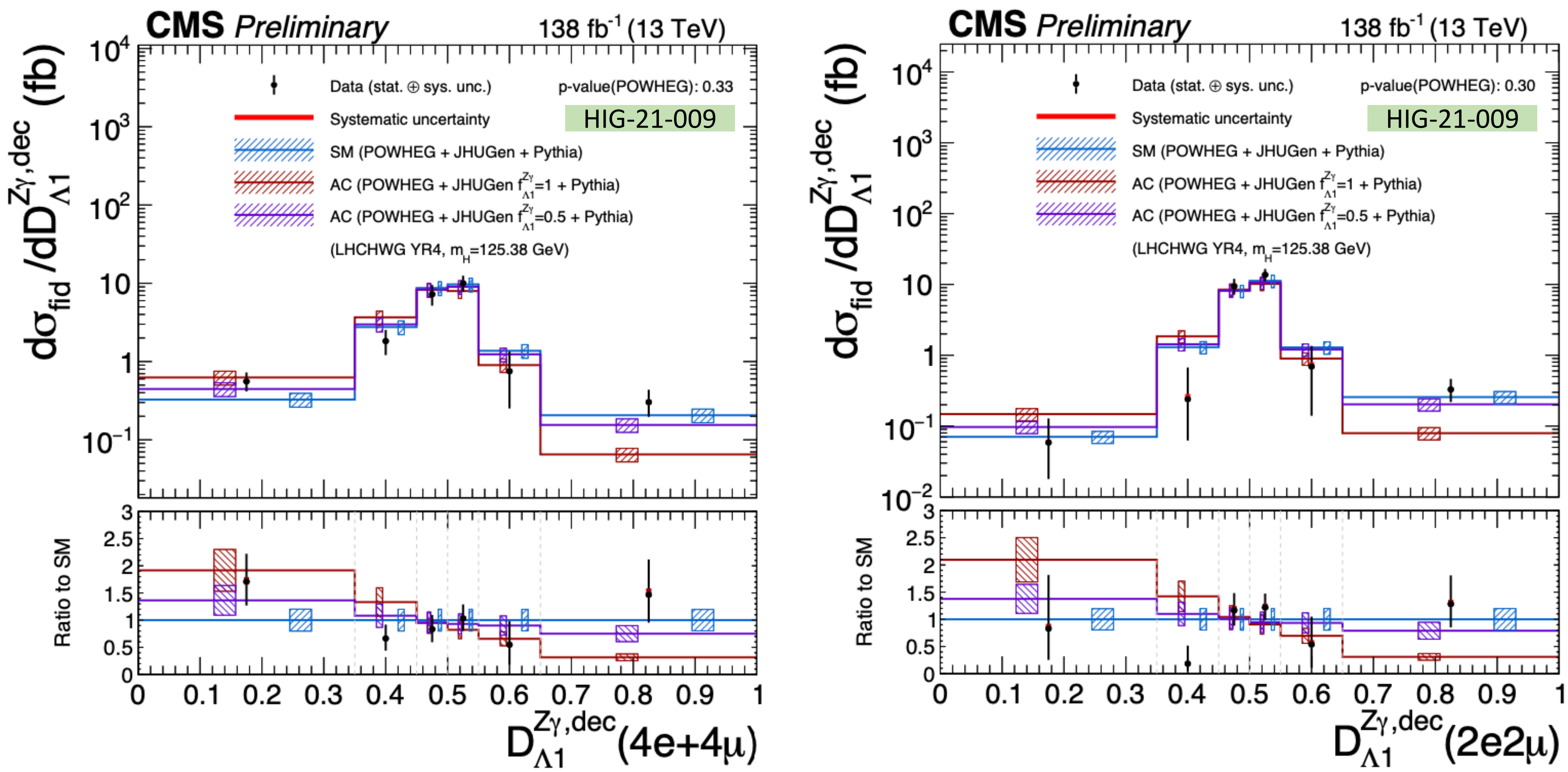

- Differential cross sections as a function of the matrix element kinematic discriminant $\mathcal{D}_{\Lambda1Z_\gamma}^{dec}(4e+4\mu)$ in the same-flavor (left) and different flavor$\mathcal{D}_{\Lambda1Z_\gamma}^{dec}(2e2\mu)$(right).

Results of measurements

Inclusive fiducial cross section

Irreducible background normalization taken from MC simulation and ZZ floating in the fit

Interpretations

k_λ, k_b, k_c

Differential observables Higgs Production

p_T^H $|y_H|$

N_{jets} p_T^{j1} p_T^{j2} m_{jj} $|\Delta\eta_{jj}|$

p_T^{Hj} m_{Hj} p_T^{Hjj} $\mathcal{T}_B$ $\mathcal{T}_C$

Differential observables Higgs decay

m_{Z1} m_{Z2}

Φ Φ_1 $\cos\theta$ $\cos\theta_1$ $\cos\theta^*$

$\mathcal{D}_{0-}^{\mathrm{dec}}$ $\mathcal{D}_{cp}^{\mathrm{dec}}$ $\mathcal{D}_{0h+}^{\mathrm{dec}}$ $\mathcal{D}_{\Lambda1}^{\mathrm{dec}}$ $\mathcal{D}_{\Lambda1}^{Z\gamma,\mathrm{dec}}$ $\mathcal{D}_{int}^{\mathrm{dec}}$

Double differential observables

m_{Z1} vs m_{Z2} N_{jets} vs p_T^H

$\mathcal{T}_C$ vs p_T^H $|y^H|$ vs p_T^H

p_T^{Hj} vs p_T^H p_T^{j1} vs p_T^{j2}

2D Differential Cross Section measurements

- A set of double differential measurements is also performed
  - Enhance sensitivity to specific phase space regions such as H+jets
  - Probe the possible BSM effects
  - Achieve a further characterization of HZZ4l
- Define mutually exclusive phase space regions for obs1 vs obs2.
- The bin boundaries for these measurements are defined with the same approach employed for one dimensional case. (The detailed bin boundaries are listed in the backup slides.)

HIG-21-009

Variable	Definition	Target
$p_T(H)$ vs $y(H)$	Transverse momentum and rapidity of the 4ℓ system	Production
m_{Z_1} vs m_{Z_2}	Invariant masses of the two Z boson candidates	Decay
$p_T(H)$ vs N_{jets}	Transverse momentum of the 4ℓ system and number of jets in the event	Production
$p_T(H)$ vs p_T^{Hj}	Transverse momenta of the 4ℓ and 4ℓ+leading jet systems	Production
p_T^{j1} vs p_T^{j2}	Transverse momenta of the leading and sub-leading jets	Production
τ_C^{jmax} vs $p_T(H)$	Transverse momenta of the Higgs and leading and τ_C^{jmax} variables	Production

Bin boundaries for 2D differential measurement

Bin	$\|y^{H}\|$	p_T^H (GeV)
Bin 1	[0,0.5]	[0, 40]
Bin 2	[0,0.5]	[40, 80]
Bin 3	[0,0.5]	[80, 150]
Bin 4	[0,0.5]	[150, ∞]
Bin 5	[0.5,1.0]	[0, 45]
Bin 6	[0.5,1.0]	[45, 120]
Bin 7	[0.5,1.0]	[120, ∞]
Bin 8	[1.0,2.5]	[0, 45]
Bin 9	[1.0,2.5]	[45, 120]
Bin 10	[1.0,2.5]	[120, ∞]

Bin	N^j	p_T^H (GeV)
Bin 1	0	[0, 15]
Bin 2	0	[15, 30]
Bin 3	0	[30, ∞]
Bin 4	1	[0, 60]
Bin 5	1	[60, 80]
Bin 6	1	[80, 120]
Bin 7	1	[120, ∞]
Bin 8	>= 2	[0, 100]
Bin 9	>= 2	[100, 170]
Bin 10	>= 2	[170, 250]
Bin 11	>= 2	[250,∞]

Bin	$\mathcal{T}_C$ (GeV)	p_T^H (GeV)
Bin 1	[0, 15]	[0, 15]
Bin 2	[0, 15]	[15, 30]
Bin 3	[0, 15]	[30, 45]
Bin 4	[0, 15]	[45, 70]
Bin 5	[0, 15]	[70, 120]
Bin 6	[0, 15]	[120, ∞]
Bin 7	[15, 25]	[0, 120]
Bin 8	[15, 25]	[120, ∞]
Bin 9	[25, 40]	[0, 120]
Bin 10	[25, 40]	[120, ∞]
Bin 11	[40, ∞]	[0, 200]
Bin 12	[40, ∞]	[200, ∞]

Bin	m_{Z_1} (GeV)	m_{Z_2} (GeV)
Bin 1	[40,85]	[12,35]
Bin 2	[40,70]	[35,65]
Bin 3	[70,120]	[35,65]
Bin 4	[85,120]	[30,35]
Bin 5	[85,120]	[24,30]
Bin 6	[85,120]	[12,24]

Bin	$p_T^{j_1}$ (GeV)	$p_T^{j_2}$ (GeV)
Bin 1	$N_{jets} < 2$	
Bin 2	[30, 60]	[30, 60]
Bin 3	[60, 350]	[30, 60]
Bin 4	[60, 350]	[60,350]

Bin	p_T^H (GeV)	p_T^{Hj} (GeV)
Bin 1	$N_{jets} < 0$	
Bin 2	[0, 85]	[0, 30]
Bin 3	[85, 350]	[0, 45]
Bin 4	[0, 85]	[30,350]
Bin 5	[85, 350]	[45, 350]

HIG-21-009

Results of 2D Differential Cross Section

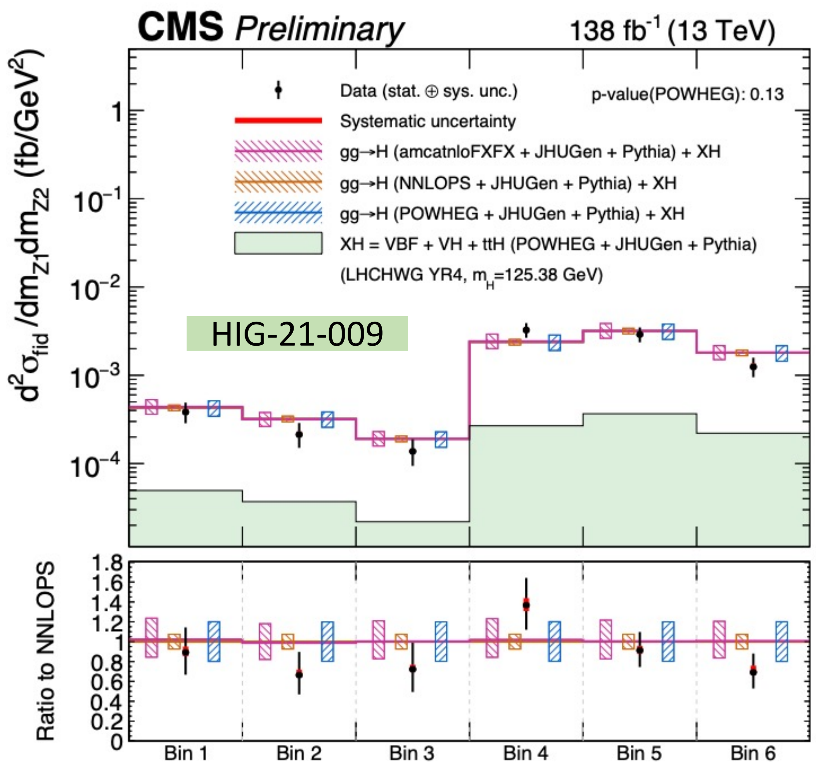

Bin	m_{Z_1} (GeV)	m_{Z_2} (GeV)
Bin 1	[40,85]	[12,35]
Bin 2	[40,70]	[35,65]
Bin 3	[70,120]	[35,65]
Bin 4	[85,120]	[30,35]
Bin 5	[85,120]	[24,30]
Bin 6	[85,120]	[12,24]

- The boundaries divide massZ1 – massZ2 plane in six regions
  - Collect the majority of signal events in several bins
  - Leave the most of background event in the other bins
  - To ensure a good S/B ratio.
- 2D Differential cross sections as a function of
  - **m_{Z1} vs m_{Z2}**

Results of 2D Differential Cross Section

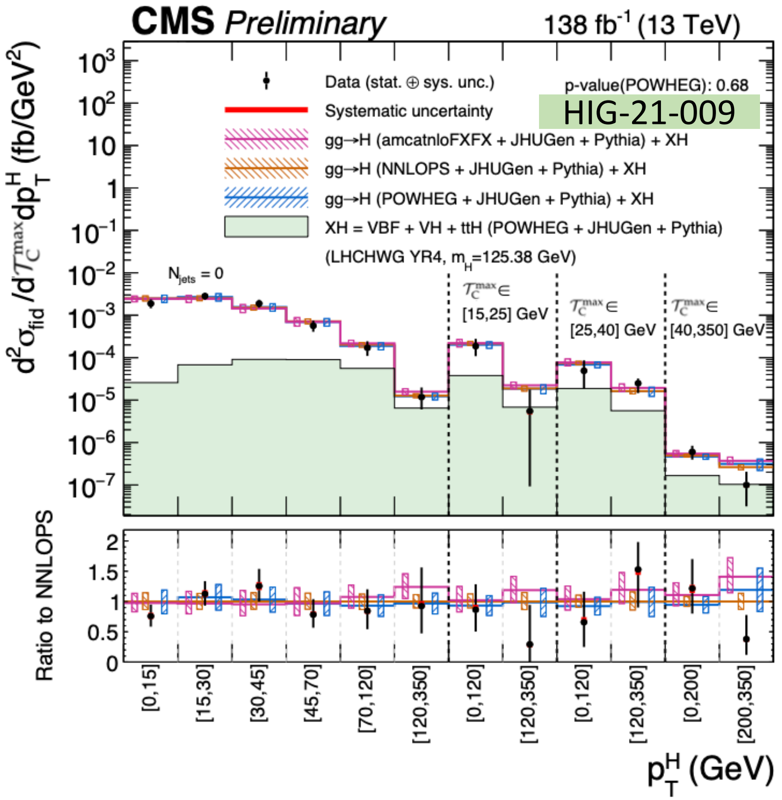

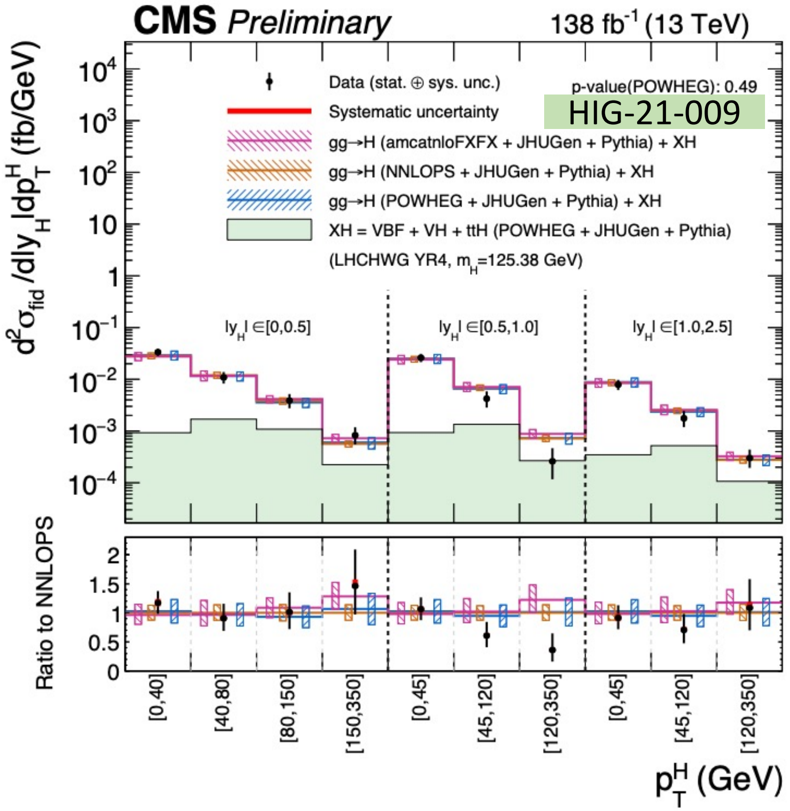

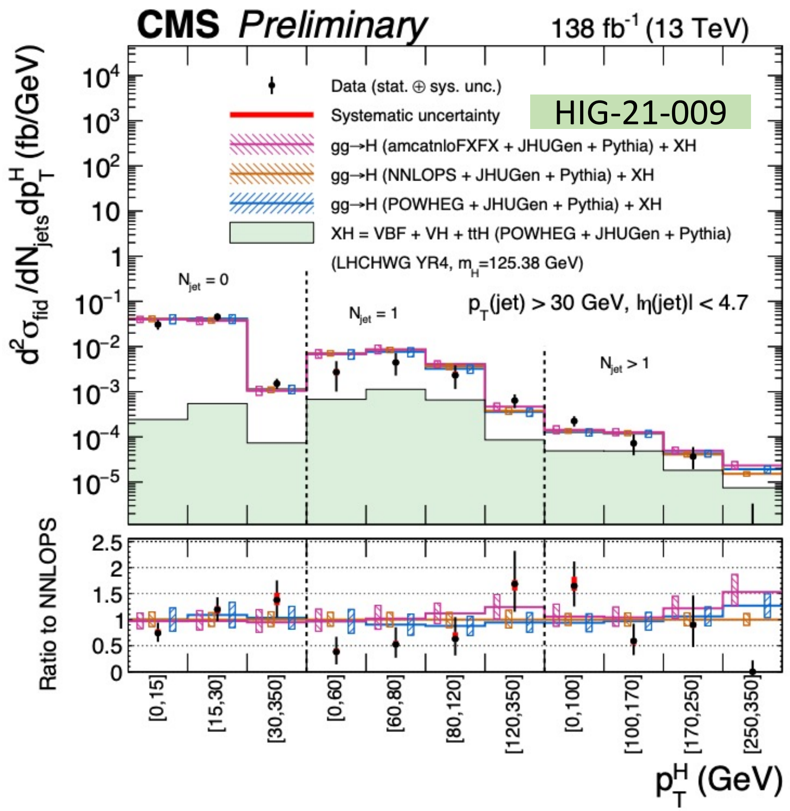

- The boundaries divide plane in regions
  - To ensure a good S/B ratio.
- 2D Differential cross sections as a function of
  - $\mathcal{T}_C$ vs p_T^H
  - $|y^H|$ vs p_T^H
  - N_{jets} vs p_T^H

Results of 2D Differential Cross Section

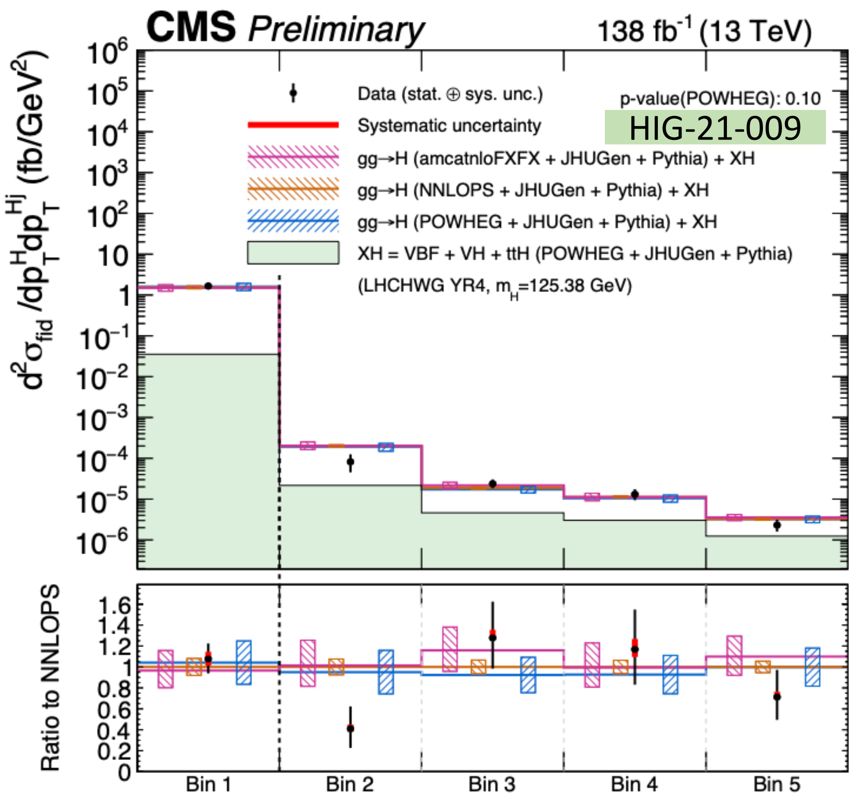

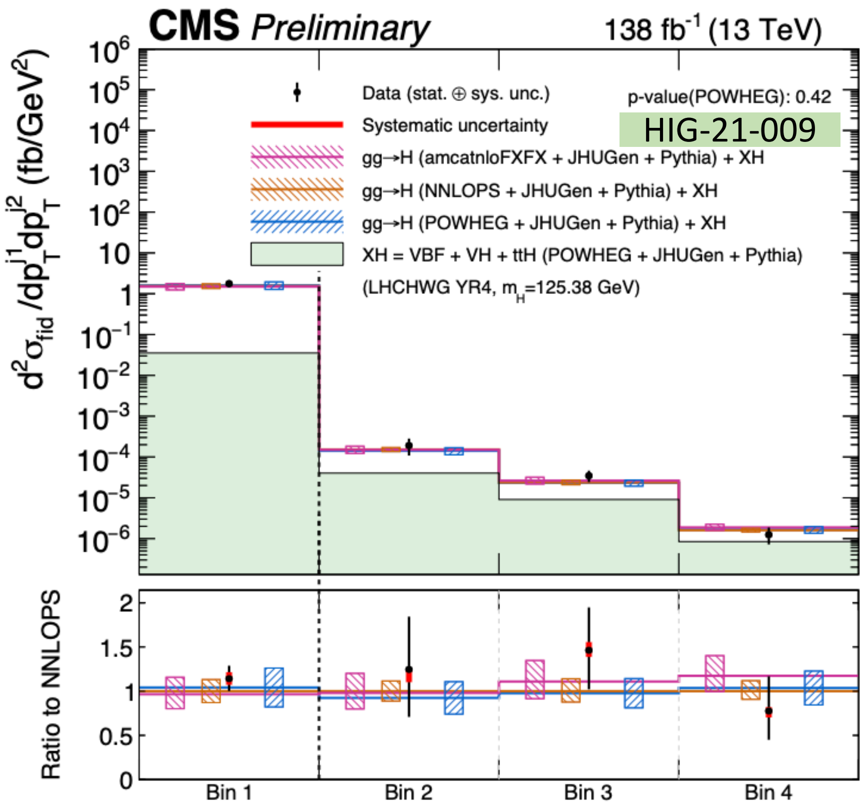

- The boundaries divide plane in regions
  - To ensure a good S/B ratio.
- 2D Differential cross sections as a function of
  - p_T^{Hj} vs p_T^H
  - p_T^{j1} vs p_T^{j2}

Bin	p_T^H (GeV)	p_T^{Hj} (GeV)
Bin 1	$N_{jets} < 1$	
Bin 2	[0, 85]	[0, 30]
Bin 3	[85, 350]	[0, 45]
Bin 4	[0, 85]	[30,350]
Bin 5	[85, 350]	[45, 350]

Bin	$p_T^{j_1}$ (GeV)	$p_T^{j_2}$ (GeV)
Bin 1	$N_{jets} < 2$	
Bin 2	[30, 60]	[30, 60]
Bin 3	[60, 350]	[30, 60]
Bin 4	[60, 350]	[60,350]

HIG-21-009

Results of measurements

Inclusive fiducial cross section

Irreducible background normalization taken from MC simulation and ZZ floating in the fit

Interpretations

k_λ, k_b, k_c

Differential observables Higgs Production

p_T^H $|y_H|$

N_{jets} p_T^{j1} p_T^{j2} m_{jj} $|\boldsymbol{\Delta\eta_{jj}}|$

p_T^{Hj} m_{Hj} p_T^{Hjj} $\mathcal{T}_B$ $\mathcal{T}_C$

Differential observables Higgs decay

m_{Z1} m_{Z2}

Φ Φ_1 $\cos\theta$ $\cos\theta_1$ $\cos\theta^*$

$\mathcal{D}_{0-}^{\text{dec}}$ $\mathcal{D}_{cp}^{\text{dec}}$ $\mathcal{D}_{0h+}^{\text{dec}}$ $\mathcal{D}_{\Lambda1}^{\text{dec}}$ $\mathcal{D}_{\Lambda1}^{Z\gamma,\text{dec}}$ $\mathcal{D}_{int}^{\text{dec}}$

Double differential observables

m_{Z1} vs m_{Z2} N_{jets} vs p_T^H

$\mathcal{T}_C$ vs p_T^H $|y^H|$ vs p_T^H

p_T^{Hj} vs p_T^H p_T^{j1} vs p_T^{j2}

Constraints on the H boson self-coupling

Probing k_λ via single-Higgs decay

- Differential XS measurement as a function of p_T^H ⇨ extract limits on H boson self coupling.

production decay

$$\mu_i^f = \mu_i \times \mu^f = \frac{\sigma^{NLO}}{\sigma^{NLO}_{SM}} \frac{BR(H\to ZZ)}{BR^{SM}(H\to ZZ)} = \frac{1+k_\lambda C_{1,i} + \delta Z_H}{(1-(k_\lambda^2-1)\delta Z_H)(1+C_{1,i}+\delta Z_H)} \times \left[1 + \frac{(k_\lambda - 1)(C_1^{\Gamma ZZ} - C_1^{\Gamma tot})}{1+(k_\lambda-1)C_1^{\Gamma tot}}\right]$$

- The cross sections of the different production mechanisms of the H boson
  - Parameterized as a function of $k_\lambda = \lambda_3/\lambda_3^{SM}$,
  - To account for NLO terms arising from the H boson trilinear self-coupling
  - Where $\delta Z_H = -1.536\times 10^{-3}$ is a universal quantity, $C_1(p_n)$ is dependent on H production model and kinematics;
  - $C_1^{\Gamma zz} = 0.0082$ and $C_1^{\Gamma tot} = 2.5\times 10^{-3}$

- $C_1 = xsec_{O(\lambda_3)}/xsec_{LO}$ by Madgraph5 simulation
- Differential predictions only for VBF, VH, and ttH
- Inclusive value for the parametrization of the H boson cross section for ggH process

Constraints on the H boson self-coupling

- Limits on k_λ extracted from a one-dimensional maximum likelihood fit:

$$S_k^{i,j}(\mu_{i,j}, \overrightarrow{\theta_s}) \rightarrow S_k^{i,j}(\mu_{i,j}(k_\lambda), \overrightarrow{\theta_s}) = \mu_{i,j}^{prod.}(k_\lambda) \times \mu^{dec}(k_\lambda) \times S_k^{i,j}(\overrightarrow{\theta_s})|_{k_\lambda=1}$$

- Different sensitivity to k_λ of each production mode
  - VBF, VH have a **mild** dependence on k_λ
  - ttH process have a very **strong** dependence on k_λ

- The observed constraint on k_λ at 68% CL is

$$k_\lambda = 4.11^{+6.41}_{-5.88} = 4.11^{+6.10}_{-5.75}(stat.)^{+1.96}_{-1.23}(syst.)$$

- The corresponding observed (expected) excluded k_λ range at 95% CL is:

$$-5.5\,(-7.7) < k_\lambda < 15.1\,(17.9)$$

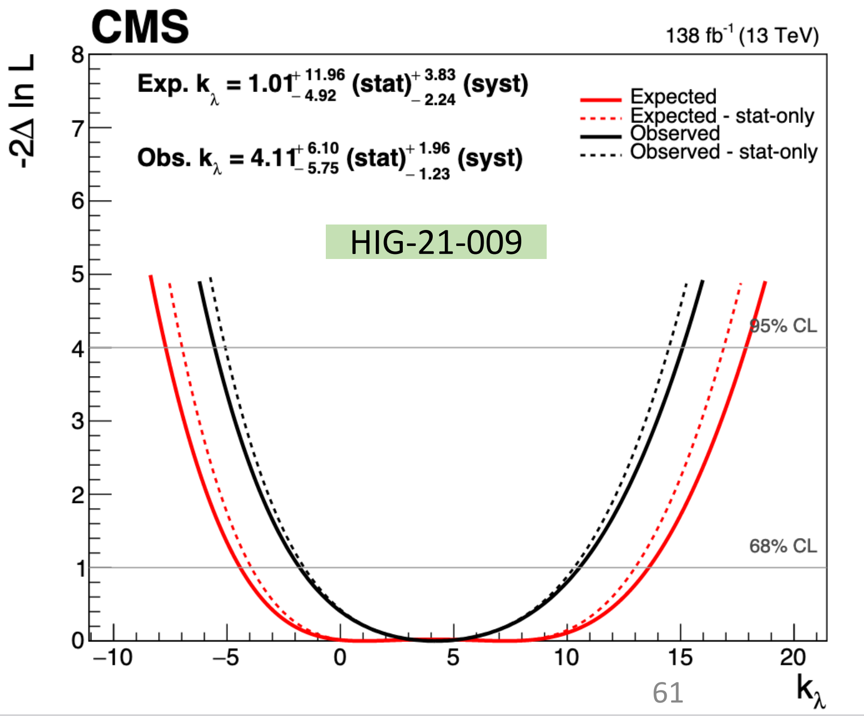

Constraints on Higgs boson couplings modifier

Probing k_b, k_c via p_T^H differential cross section

- Interpretation of p_H^T ⇨ extract limits of Higgs boson coupling of light quarks

- Described in κ – framework
  - Coupling modifiers expressed as $\kappa_c = y_c / y_c^{SM}$
  - Scan of modification κ_c
  - Check its relative formula with P_H^T distribution

- The theory predication combined of 2 method
  - Loop-induced ggF production -- Radish
  - Quark-initiated production of Higgs

    -- MadGraph5_aMC@NLO

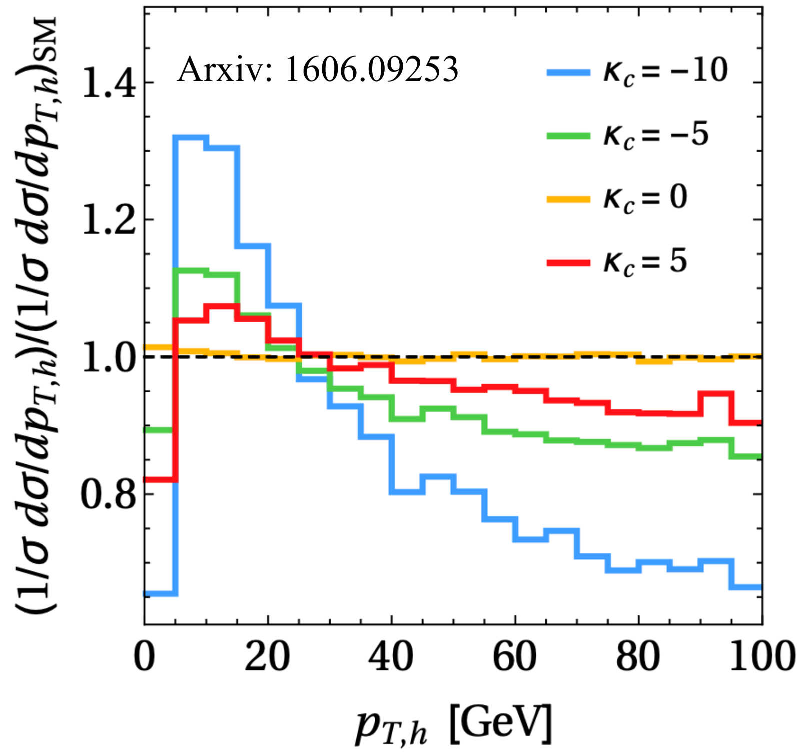

Two methods applied in the constrain of κ_b κ_c

- Results vary strongly depending on the assumption of the **branching ratios**.
- **Overall discrimination** power
  - **Shape**
  - **Normalization**
- ***The branching ratios depend on the couplings***
  - Maximum amount of discrimination power
  - Normalization
    - Expected **Cross section**
    - **Branching ratios** scaled with coupling modifications
    - Constrain by the **Higgs decay width**.
- ***Freely floating branching ratios***
  - Normalization of parametrization and coupling dependence of BRs are **eliminated**
  - **Purely the constraints from only the shape**.

Comparison of κ_b VS κ_c

HIG-21-009		Full Run2 Ultra Legacy Floating κ_b κ_c	
		Observed 95% confidence interval	**Expected** 95% confidence interval
Shape-Only	κ_b	[-5.6, 8.9]	[-5.5, 7.4]
	κ_c	[-20, 23]	[-19, 20]
Shape+ normalization	κ_b	[-1.1, 1.1]	[-1.3, 1.2]
	κ_c	[-5.3, 5.2]	[-5.7, 5.7]

	Direct measurement via $(W/Z)H \to c\bar{c}$	
	CMS 95% confidence interval	**ATLAS** 95% confidence interval
κ_c	1.1<|κ_c|<5.5 (|κ_c|<3.4)	|κ_c|<8.5 (12.4)
	arxiv:2205.05550	Eur. Phys. J. C (2022) 82:717

- Observed and expected constraints in 95% confidence intervals for the Yukawa coupling modifiers
- (Left) Indirect measurement by p_T^H in $H \to ZZ \to 4l$
  - Simultaneous fit for coupling modifier κ_b, κ_c assuming
  - (Top) coupling dependence of the branching fractions (*shape+normalization*)
  - (Bottom)branching fractions implemented as nuisance parameters with no prior constraint (*shape-only*)
- (Right) Direct measurement of κ_c via $H \to c\bar{c}$ of ATLAS and CMS
- When the κ_b is fixed to SM, the κ_c region of shape+normalization would be **almost half** of the value in left table, which is also confirmed by ATLAS indirect measurement[CERN-EP-2022-143]
- Compared with the direct measurement of κ_c via $H \to c\bar{c}$, the expected results achieve the agreement at CMS